STATE OF FLORIDA

Use of Nondestructive Techniques to Estimate the Allowable Vibratory Compaction Level during Construction

Research Report
FL/DOT/SMO/07-BDB-11

N. Mike Jackson, Ph.D., P.E.
Michael I. Hammons, Ph.D., P.E.
Robert Walker
Harold Von Quintus, P.E.

March 31, 2007

STATE MATERIALS OFFICE

DISCLAIMER

The opinions, findings, and conclusions expressed in this publication are those of the authors and not necessarily those of the State of Florida Department of Transportation.

SI* (MODERN METRIC) CONVERSION FACTORS

APPROXIMATE CONVERSIONS TO SI UNITS

SYMBOL	WHEN YOU KNOW	MULTIPLY BY	TO FIND	SYMBOL
LENGTH				
in	inches	25.4	millimeters	mm
ft	feet	0.305	meters	m
yd	yards	0.914	meters	m
mi	miles	1.61	kilometers	km

SYMBOL	WHEN YOU KNOW	MULTIPLY BY	TO FIND	SYMBOL
AREA				
in^2	squareinches	645.2	square millimeters	mm^2
ft^2	squarefeet	0.093	square meters	m^2
yd^2	square yard	0.836	square meters	m^2
ac	acres	0.405	hectares	ha
mi^2	square miles	2.59	square kilometers	km^2

SYMBOL	WHEN YOU KNOW	MULTIPLY BY	TO FIND	SYMBOL
VOLUME				
fl oz	fluid ounces	29.57	milliliters	mL
gal	gallons	3.785	liters	L
ft^3	cubic feet	0.028	cubic meters	m^3
yd^3	cubic yards	0.765	cubic meters	m^3
NOTE: volumes greater than 1000 L shall be shown in m^3				

SYMBOL	WHEN YOU KNOW	MULTIPLY BY	TO FIND	SYMBOL
MASS				
oz	ounces	28.35	grams	g
lb	pounds	0.454	kilograms	kg
T	short tons (2000 lb)	0.907	megagrams (or "metric ton")	Mg (or "t")

SYMBOL	WHEN YOU KNOW	MULTIPLY BY	TO FIND	SYMBOL
TEMPERATURE (exact degrees)				
^oF	Fahrenheit	5 (F-32)/9 or (F-32)/1.8	Celsius	^oC

SYMBOL	WHEN YOU KNOW	MULTIPLY BY	TO FIND	SYMBOL
ILLUMINATION				
fc	foot-candles	10.76	lux	lx
fl	foot-Lamberts	3.426	candela/m^2	cd/m^2

SYMBOL	WHEN YOU KNOW	MULTIPLY BY	TO FIND	SYMBOL
FORCE and PRESSURE or STRESS				
lbf	poundforce	4.45	newtons	N
lbf/in^2	poundforce per square inch	6.89	kilopascals	kPa

APPROXIMATE CONVERSIONS TO SI UNITS

SYMBOL	WHEN YOU KNOW	MULTIPLY BY	TO FIND	SYMBOL
		LENGTH		
mm	millimeters	0.039	inches	in
m	meters	3.28	feet	ft
m	meters	1.09	yards	yd
km	kilometers	0.621	miles	mi

SYMBOL	WHEN YOU KNOW	MULTIPLY BY	TO FIND	SYMBOL
		AREA		
mm^2	square millimeters	0.0016	square inches	in^2
m^2	square meters	10.764	square feet	ft^2
m^2	square meters	1.195	square yards	yd^2
ha	hectares	2.47	acres	ac
km^2	square kilometers	0.386	square miles	mi^2

SYMBOL	WHEN YOU KNOW	MULTIPLY BY	TO FIND	SYMBOL
		VOLUME		
mL	milliliters	0.034	fluid ounces	fl oz
L	liters	0.264	gallons	gal
m^3	cubic meters	35.314	cubic feet	ft^3
m^3	cubic meters	1.307	cubic yards	yd^3

SYMBOL	WHEN YOU KNOW	MULTIPLY BY	TO FIND	SYMBOL
		MASS		
g	grams	0.035	ounces	oz
kg	kilograms	2.202	pounds	lb
Mg (or "t")	megagrams (or "metric ton")	1.103	short tons (2000 lb)	T

SYMBOL	WHEN YOU KNOW	MULTIPLY BY	TO FIND	SYMBOL
		TEMPERATURE (exact degrees)		
^oC	Celsius	1.8C+32	Fahrenheit	^oF

SYMBOL	WHEN YOU KNOW	MULTIPLY BY	TO FIND	SYMBOL
		ILLUMINATION		
lx	lux	0.0929	foot-candles	fc
cd/m^2	candela/m^2	0.2919	foot-Lamberts	fl

SYMBOL	WHEN YOU KNOW	MULTIPLY BY	TO FIND	SYMBOL
		FORCE and PRESSURE or STRESS		
N	newtons	0.225	poundforce	lbf
kPa	kilopascals	0.145	poundforce per square inch	lbf/in^2

*SI is the symbol for the International System of Units. Appropriate rounding should be made to comply with Section 4 of ASTM E380. (Revised March 2003)

Technical Report Documentation Page

1. Report No.	2. Government Accession No.	3. Recipient's Catalog No.
4. Title and Subtitle **Use of Nondestructive Techniques to Estimate the Allowable Vibratory Compaction Level during Construction**		5. Report Date **March 31, 2007** 6. Performing Organization Code
7. Author(s) **N. Mike Jackson, Michael I. Hammons, Robert Walker, and Harold Von Quintus**		8. Performing Organization Report No. **FL/DOT/SMO/07-BDB-11**
9. Performing Organization Name and Address **University of North Florida 4567 St. Johns Bluff Rd., South Jacksonville, FL 32224**		10. Work Unit No. (TRAIS) 11. Contract or Grant No. **BDB-11**
12. Sponsoring Agency Name and Address **Florida Department of Transportation 605 Suwannee St. MS 30 Tallahassee, Florida 32399 (850)414-4615**		13. Type of Report and Period Covered **Final Report** 14. Sponsoring Agency Code
15. Supplementary Notes		

16. Abstract

Earthborne vibrations from vibratory compaction equipment can be described as single-frequency continuous vibration. Human perception of ground vibrations is subjective and depends upon a number of factors. Damage to structures caused by earthborne vibrations can be categorized as either architectural or structural damage. Architectural damage is superficial damage such as hairline cracks in plaster walls or ceilings. While catastrophic damage to buildings from construction operations are extremely rare, some structural damage such as separation of masonry blocks and cracking in foundations, and other sensitive structures may occur in cases where earthborne vibrations exceed threshold levels. Various Federal, State, and foreign agencies have proposed vibration limit criteria, some intended to mitigate damage to structures, while others are based upon limiting human annoyance. Two of these existing criteria were selected to form the basis of the recommendations documented herein. These criteria are represented as three zones on a plot of peak particle velocity versus vibratory roller frequency. A square root scaling law of ground motion is used to predict the ground motions from vibratory compaction equipment from FWD data. A potentially vibration-sensitive portion of a project can be identified using displacement-time histories from the FWD obtained during routine pre-construction testing. Detailed knowledge of the layering of the pavement structure or the geology of the surrounding site is not required. It is demonstrated that this predictor can be used to restrict vibratory compaction near sensitive structures and fragile buried infrastructure.

17. Key Word	18. Distribution Statement
Vibratory roller, FWD, Ground motion, Pre-construction testing, Displacement-time histories, Peak particle velocity, Prediction model, Buried infrastructure.	**No Restrictions**

19. Security Classif. (of this report)	20. Security Classif. (of this page)	21. No. of Pages	22. Price
Unclassified	**Unclassified**	**80**	

Form DOT F 1700.7 (8-72) Reproduction of completed page authorized

EXECUTIVE SUMMARY

The Superpave™ mixture design method was developed under the Strategic Highway Research Program (SHRP). During the early stages of the Superpave™ implementation effort, few problems were encountered while producing the mix. However, obtaining density on the roadway was a consistent problem across the U.S. and higher density specifications have generally been implemented by highway agencies. Larger vibratory rollers are often used because of their efficiency. However, greater ground motion caused by these vibratory rollers have been suspected of potentially resulting in damage to adjacent infrastructure, particularly in or near urban areas.

Earthborne vibrations from vibratory compaction equipment can be described as single-frequency continuous vibration. Human perception of such ground vibrations is subjective and depends upon a number of factors. Damage to structures caused by these earthborne vibrations can be categorized as either architectural or structural damage. Architectural damage is superficial damage such as hairline cracks in plaster walls or ceilings. While catastrophic damage to buildings from construction operations are extremely rare, some structural damage such as separation of masonry blocks and cracking in foundations, and other sensitive structures may occur in cases where earthborne vibrations exceed threshold levels.

Various Federal, State, and foreign agencies have proposed vibration limit criteria, some intended to mitigate damage to structures, while others are based upon limiting human annoyance. Two of these existing criteria (the U.S. Office of Surface Mines blasting level criteria, and the German DIN 4150 Standard level for human annoyance) were selected to form the basis of the recommendations documented herein. These criteria are used to differentiate three zones on a plot of peak particle velocity versus vibratory roller frequency.

A square root scaling law of ground motion is used to predict the ground motions from vibratory compaction equipment based on FWD data. With this predictor, a potentially vibration-sensitive portion of a resurfacing project can be identified using displacement-time histories from the FWD obtained during routine pre-construction testing. Detailed knowledge of the layering of the pavement structure or the geology of the surrounding site is not required. It is demonstrated herein with that this predictor can successfully be used to restrict vibratory compaction near sensitive structures, including fragile buried infrastructure.

TABLE OF CONTENTS

LIST OF FIGURES

LIST OF TABLES

1 INTRODUCTION

1.1 Background

The Superpave^{TM} mixture design method was developed under the Strategic Highway Research Program (SHRP). During the early stages of the Superpave^{TM} implementation effort, few problems were encountered while producing the mix. However, obtaining density on the roadway has proved to be a consistent problem across the U.S. and higher density specifications have been implemented by highway agencies.

Density is used by the Florida Department of Transportation (FDOT) for acceptance of HMA mixtures on the roadway and is targeted by most contractors for controlling the paving operation. To achieve a higher level of in-place density, a combination of static and vibratory rollers is typically used today. Large vibratory rollers are often used because of their efficiency. However, greater ground motion caused by these vibratory rollers may induce damage to adjacent infrastructure, particularly in or near urban areas.

The majority of flexible pavement design projects in Florida consist of rehabilitations of existing roadways. FDOT uses the 1993 AASHTO pavement design procedure (AASHTO 1993) tailored for Florida conditions (FDOT 2004). Most rehabilitation projects require that the design engineer evaluate the structural capacity of the existing roadway and select a structural overlay thickness such that the pavement structure will maintain the desired serviceability over the design life.

Preliminary pre-design data are from a number of sources including the Pavement Condition Survey (PCS), the Roadway Characteristics Index (RCI), skid data, Straight Line Diagrams (SLD), and old plans. Prior to developing the rehabilitation design, the engineer must gather detail design parameters that are direct inputs into the structural design procedure. These parameters include a description of the design traffic ($ESAL_D$), existing layer types and thicknesses, distresses, and an assessment of the design resilient modulus (M_R) of the subgrade soils. Because the subgrade soils can be highly variable and are affected by moisture, the resilient modulus may be highly variable within the project limits: thus, the design M_R is calculated to represent a practical design value within the project limits.

The FDOT preferred method to obtain M_R is by using the FWD (Holzschuher and Lee 2007. The FWD device consists of an impact loading mechanism and a set of sensors to measure vertical surface displacements under the load and at specified offsets from the load. The loading device consists of a load plate that can apply an impulse load of different magnitudes ranging from 1,500 to 27,000 lbs. The load can be applied from three standard drop heights resulting in a load pulse of 0.025 to 0.03 seconds. Figure 1 shows a typical time-history of a 9000-lbs magnitude FWD load pulse. The load plate is circular and has a standard diameter of 11.8 inches.

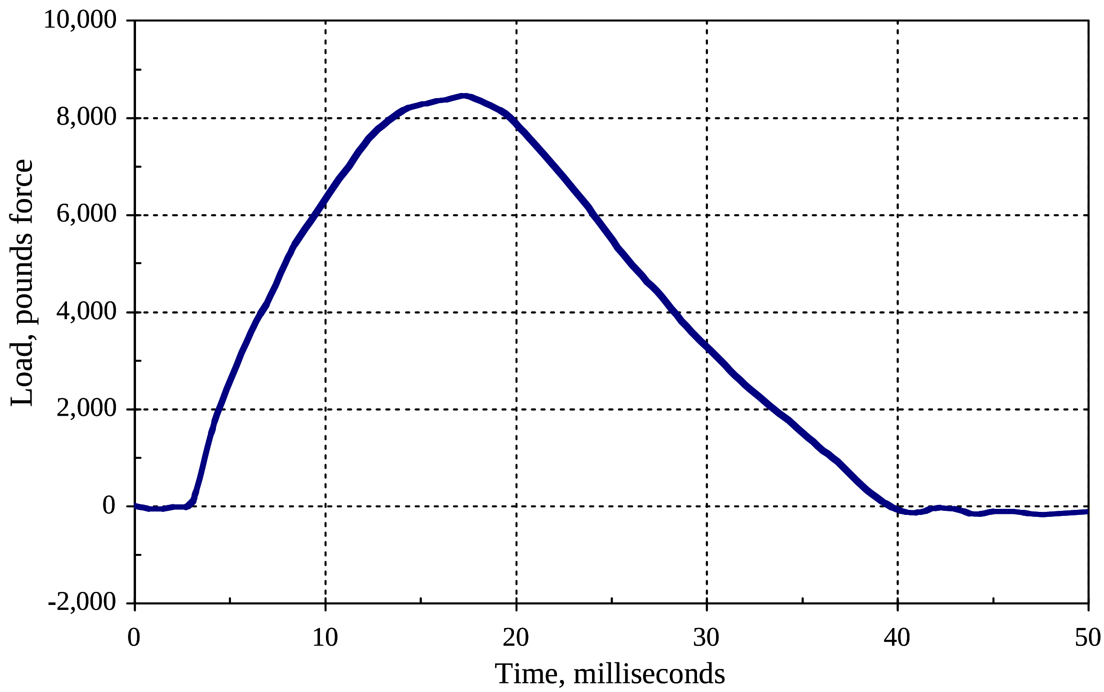

Figure 1-1. Typical FWD load-time history

The procedure adopted by FDOT prescribes test spacing, number and magnitude of the impulsive load, and the method to calculate M_R. For two lane roadways 28 tests are conducted per mile (one way). For multilane roadways 14 tests per mile are conducted each way. An approximately 9000-lb load is applied twice at each test location. The first drop is a seating load, and data from this drop are not used in the analysis. The second drop is executed, and data from this load are used to calculate the embankment M_R at that point. Figure 1-2 shows the FWD configuration used by FDOT.

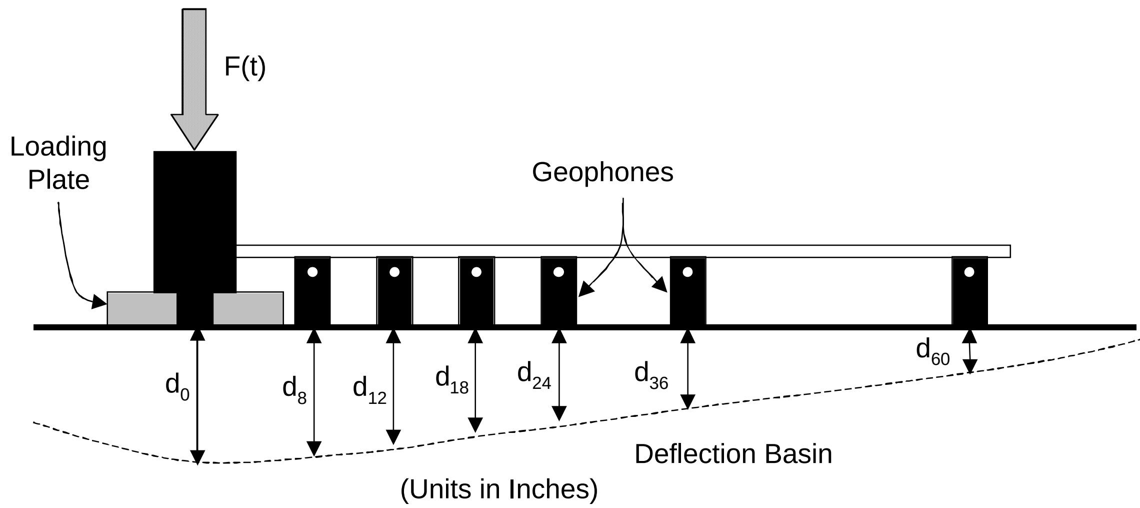

Figure 1-2 FWD configuration for pre-design evaluation

The design M_R is calculated using the following equation based upon Boussinesq theory and the variability of the calculated resilient modulus values with the project limits:

$$M_R = \frac{0.24\overline{P}}{\left(\overline{d}_{36} + 1.96\sigma_{36}\right)36} \qquad \text{(Equation 1-1)}$$

where P is the average load in lbs, d_{36} is the average deflection at the sensor 36 inches from the center of the impulsive load, and σ_{36} is the standard deviation of the load at 36 inches from the center of the load. The maximum allowable M_R allowed by FDOT is 32,000 psi. These values typically occur where limestone or coral is located very close to the surface.

1.2 Objective

The objective of this study was to develop a practical methodology to identify areas where vibratory compaction is not recommended during construction of Hot Mix Asphalt (HMA) pavements based on FWD data obtained as a part of the preliminary design study. Both vibratory drum rollers and the FWD device apply impact loads to pavements. The FWD device employs an impulse load by dropping weights from pre-determined heights, while vibratory compactors continuously apply impact loads at a given vibration frequency. Therefore, it is envisioned that it may be possible to use the FWD device to predict the effect of vibratory compactor on the adjacent structures or buried systems.

1.3 Scope

The research project began with a comprehensive literature search to review wave propagation in geologic media and to identify vibration criteria which may be applicable to the vibratory compaction. This was followed by an analytical study designed to develop a method to relate measured FWD response to peak vibration expected for typical Florida conditions (sandy soil with high water table). The results of the analytical study were used to develop a model to predict a “go” or “no go” condition for dynamic compaction of Superpave™ mixes. Finally, the model was verified by comparison to actual ground motion data obtained during compaction.

2 LITERATURE REVIEW

2.1 Physics of Earthborne Vibrations

2.1.1 Wave Types

Vibrations propagate through geologic media in response to natural or man-made phenomena such as earthquakes, explosions, machinery, and traffic (Hendriks 2002). A complex wave pattern is created as energy reflects and refracts off the ground surface and subsurface interfaces between dissimilar materials (Dowding 1996). To simplify the description of these complex phenomena, the effects of the waves are typically described by the time history of the motion of a soil particle of interest. As energy passes the soil particle, it is forced to move in a complex three-dimensional manner. Three principal wave types describe earthborne vibrations:

- Compression or p-waves are body waves that expand from the energy source along a spherical wave front. The particle motion from this type of wave is along the direction of expanding wave front in a "push-pull" manner.

- Shear or s-waves are also body waves expanding along a spherical wave front. However, particle motion is perpendicular (transverse) to the direction of wave propagation.

- Surface or Rayleigh waves travel along the ground surface. These waves expand along a cylindrical wave front, analogous to ripples formed by dropping a pebble into a body of water. The particle motion is a retrograde ellipse in a vertical plane resulting in motion both along and perpendicular to the direction of wave propagation. Rayleigh wave motion penetrates the ground surface a distance of only one to two wavelengths.

A number of descriptors of soil particle motion could be used: particle displacement, particle velocity, and particle acceleration (Hendriks 2002). The most useful measure is usually particle velocity. Tracking the direction of motion of the soil particle is important in interpreting the nature of the wave or waves causing the motion. Components of particle velocity in three dimensions (vertical, horizontal, and transverse) can be described by the peak particle velocity (PPV) or by a true vector sum. For most construction vibration problems, the PPV, defined as the maximum velocity component, is used as a descriptor of the effects of the wave (Dowding 1996). There may be times when the true vector sum is larger in magnitude than the PPV, but this usually occurs at the same time as the PPV. Note that PPV should not be confused with wave propagation velocity.

The wave propagation velocity of the compression wave is larger than that of the shear wave, and the Rayleigh wave is even slower. Thus, the first wave to arrive at a point on or near the surface will be the compressive wave, followed in succession by the shear wave and the Rayleigh wave (Dowding 1996).

2.1.2 Wave Attenuation

Vibrations from construction equipment propagate through the soil to a distant receiver predominantly by means of Rayleigh waves and secondarily by means of body waves (Amrick and Gendreau 2000). The amplitude of these waves decreases with distance from the source. Attenuation of earthborne vibrations is due to two phenomena: geometrical attenuation and material damping. Geometrical attenuation can be described by the spreading of the wave energy over an ever-increasing wave front surface. As the wave propagates, there is a corresponding decrease in energy per unit area of the expanding wave surface. Material or hysteretic damping occurs as non-recoverable processes such as friction consume a portion of the energy.

Combined geometric and material damping of waves can be described by the relationship

$$v_b = v_a \left(\frac{r_a}{r_b} \right) e^{\alpha (r_a - r_b)} \qquad \text{(Equation 2-1)}$$

where v_b is the particle velocity at distance r_b and v_a is the particle velocity at distance r_a. The coefficient γ is the geometric attenuation coefficient and depends upon the propagation mechanism. Table 2-1 lists the theoretical geometric attenuation coefficients for the various wave types.

Table 2-1. Theoretical geometric attenuation coefficients (Amick and Gendreau 2000)

Source	Wave Type	Measurement Point	γ
Point on surface	Rayleigh	Surface	0.5
Point on surface	Body	Surface	2
Point at depth	Body	Surface	1
Point at depth	Body	Depth	1

The material coefficient α depends upon the frequency of the wave and the type of material. In general, α is greater at higher frequencies and for stiffer materials. Amick (1999) has proposed a frequency-dependent soil propagation model in which α is dependent upon the frequency, commonly referred to as a non-linear soil propagation model. However, over the range of frequencies common to construction vibrations, α is often assumed to be independent of frequency and to be related only to the type of material (Hendriks 2002). Table 2-2 presents a listing of published material attenuation coefficients.

Table 2-2. Summary of published material attenuation coefficients (Amick and Gendreau 2000)

Investigator	Soil Type	Material Coefficient, α, m^{-1}
Forssblad	Silty gravelly sand	0.13
Richart	4-6 inches concrete slab over compacted granular fill	0.02
Woods	Silty fine sand	0.26
Barkan	Saturated fine grain sand	0.1
	Saturated sand with laminae of peat and organic silt	0.04
	Clayey sand, clay with some sand, and silt above water level	0.04
	Saturated clay with sand and silt	0.0-0.12
Dalmatov, et al.	Sand and silts	0.026-0.36
Clough and Chameau	Sand fill over bay mud	0.05-0.2
	Dune sand	0.026-0.065
Peng	Soft Bangkok clay	0.026-0.44

Figure 2-1 shows an example of Rayleigh wave attenuation for selected attenuation coefficients. An attenuation coefficient α = 0.001 m^{-1} is representative of a hard, competent rock, while α = 0.01 m^{-1} is representative of a hard soil, and α = 0. 1 m^{-1} is representative of weak or soft soil. Thus, as expected, Rayleigh wave attenuation is much more pronounced in weak soils than in more competent materials.

Often, it is assumed that material damping is small compared to geometric damping; thus, it follows from Equation 2-1 and Table 2-1 that geometric damping dictates that Rayleigh wave particle velocity on the surface decreases with the square root of radius.

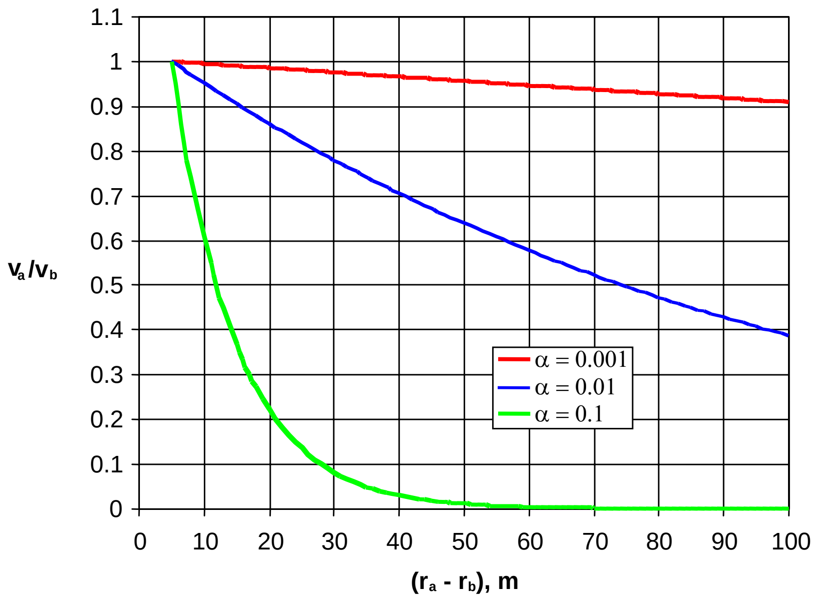

Figure 2-1. Attenuation of Rayleigh wave with distance for selected material attenuation coefficient

Rayliegh waves decay exponentially with depth. The depth of penetration of the wave is approximately equal to its wavelength, which is a function of the wave velocity of the material and frequency of the wave. The decay in wave amplitude with depth is given by the following relationship:

$$A(z) = A_0 e^{-z/z_o} \qquad \text{(Equation 2-2)}$$

where $A(z)$ = Rayleigh wave amplitude at depth z

A_o = Amplitude at the surface

z_o = characteristic penetration depth (proportional to wavelength)

If we assume a wave velocity of 15,000 in/sec (a value typical of a dense, unsaturated sand), we obtain the curves in Figure 2-2. This chart indicates the amplitude of the wave has decreased by about 50 percent at a depth of approximately 50 inches.

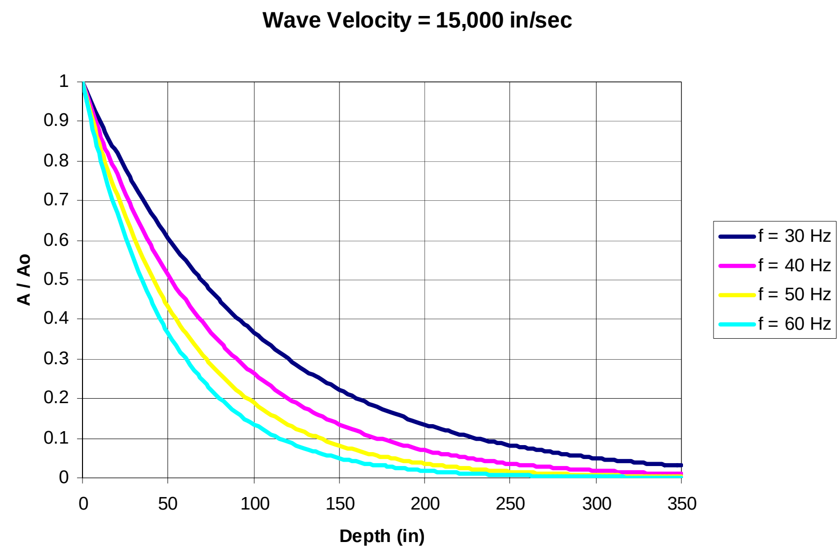

Figure 2-2. Attenuation of Rayleigh waves with depth for dense, unsaturated sand

2.1.3 Vibration Characteristics

Vibrations may be further characterized into one of two types: 1) finite cycle (transient) vibrations, and 2) infinite cycle (continuous) vibrations (Hendriks 2002). Vibrations from high energy, short duration phenomena such as blasting, pile driving, and dynamic compaction are transient vibrations, while continuously vibrating stationary machinery produces steady state, harmonic motion consisting of a near infinite number of similarly shaped pulses. Transient vibrations do not tend to excite resonance in undamped or lightly damped structures, as do continuous harmonic motions near the structure's fundamental frequency. Nonetheless, transient vibrations are of concern, because under the right conditions, they can cause architectural or structural damage.

Amick and Gendreau (2000) have characterized the following four categories of construction vibration:

- *Continuous random vibration*. Vibrations may cover a wide frequency range. Most excavation and static compaction equipment fall into this category. Tracked vehicles are commonly of this type, but may also exhibit characteristics of high-rate repeated impaction due to tracks impacting the ground surface.
- *Random vibrations due to single impact or low-rate repeated impact*. This type of vibration results in soil "ringing" due to sudden dynamic loading. It may include pile driving, blasting, use of a drop ball, or FWD testing.
- *High-rate repeated impact*. This type is typified by the jackhammer, which generates vibrations at the frequency of impact (such as 19 Hz) and integer multiples of that rate (such as 38 Hz, 57 Hz, etc.)

- *Single-frequency continuous vibration*. The predominant sources of this type of vibration are vibratory pile driving, pile extraction, and vibratory compaction. They are similar to sinusoidal vibration.

2.2 Vibration Effects

2.2.1 Human Annoyance

While the vibration level required to cause building damage is far greater than the threshold of human perception, several state DOTs familiar with the backlash that can occur with construction projects have learned to show sensitivity to public perception (CTC and Associates LLC 2003).

Human perception of ground vibrations is subjective and depends upon a number of factors. It is recognized that a person working in a factory is likely less sensitive to vibration than that same person would be quietly reading a book in a residence. Most routine complaints of vibration come from persons who are ill, elderly, or are engaged in a vibration sensitive hobby or activity. Even low level vibrations may cause annoying secondary effects such as rattling of windows, doors, or dishes. While these secondary vibrations may be irritating, they are not likely to cause property damage (Hendriks 2002).

2.2.2 Buildings

2.2.2.1 <u>Architectural Damage</u>

Architectural damage is superficial damage such as hairline cracks in plaster walls or ceilings. Most buildings usually have residual strains as a result of foundation movement, moisture and temperature cycles, poor maintenance, or past construction activities. In some cases, even relatively small levels of vibrations can result in superficial damage (Hunaidi 2000). In other cases, properties owners may have failed to notice pre-existing superficial damage until after a vibration event occurs. In such cases, it may be impossible to prove that the damage was not a result of the construction operations.

2.2.2.2 <u>Structural Damage</u>

While catastrophic damage to buildings from construction operations are extremely rare, some structural damage such as separation of masonry blocks and cracking in foundations, swimming pools, chimneys, and other sensitive structures may occur in cases where earthborne vibrations exceed threshold levels.

2.2.3 Buried Infrastructure

Approximately 80% of the ground motion energy goes to producing surface waves, and this energy propagates as a cylindrical wave. As indicated in Section 2.1.2, the amplitude of these surface waves decreases exponentially with depth. The pressure (body) wave is of very low amplitude, and looses amplitude rapidly from geometric attenuation as it propagates as a volumetric wave.

Any subterranean flexible structures, such as communication cables, are not distressed by typical construction vibrations. Brittle structures are more difficult to predict, and their backfill environment will likely be the key issue. In general culverts, conduits and pipes are not susceptible to mild ground shock. The weak link in these structures tends to be the joints of the connecting pipe, which may be distressed due to possible settlement from the sustained vibration of the repeated passing of the vibratory roller.

2.3 Vibration Limit Criteria

Federal, State, and foreign agencies have proposed various vibration limit criteria. Some criteria are intended to mitigate damage to structures, while others are based upon limiting human annoyance. In this section, we summarize the most important vibration limit criteria found in the literature

2.3.1 Transient Event Criteria

Construction vibrations such as blasting and pile driving are generally considered to be transient events. Most criteria for this type of phenomena have been developed for applications to buildings in close proximity to surface mines where excavation by blasting is common.

2.3.1.1 U.S. Office of Surface Mining (OSM)

The most often cited empirical blast vibration damage criteria for residential construction was published by the U.S. Bureau of Mines after a decade-long research program to measure and evaluate earthborne blast vibrations and their effects on structures (Nichols et al 1971). This document recommended a criterion of a peak particle velocity of 2 in/sec regardless of the frequency of vibration. About a decade later, additional research by Siskind et al (1980) recommended that this criterion be modified by reducing the maximum allowable particle velocity for vibration frequencies less than 40 Hz. Even later, the OSM issued a regulation providing guidance for safe levels of surface blasting for typical residential structures. The graph shown in Figure 2-3 is a revision of frequency-based safe limits for cosmetic cracking published in U.S. Bureau of Mines in RI 8507 (Siskind et al 1980). The RI 8507 study was focused on preventing architectural damage such as cosmetic cracking in low-rise residential structures adjacent to surface mines. No distinction is made concerning the type construction or age of the building.

The OSM criteria recognize four dominant frequency ranges: 1 to 3.5 Hz, 3.5 to 12 Hz, 12 to 30 Hz, and 30 to 100 Hz. Svinkin (2005) reports that the RI 8507 study involved no direct measurements of blasts with dominant frequencies below 5 Hz or and few construction blasts with dominant frequencies above 30 Hz.

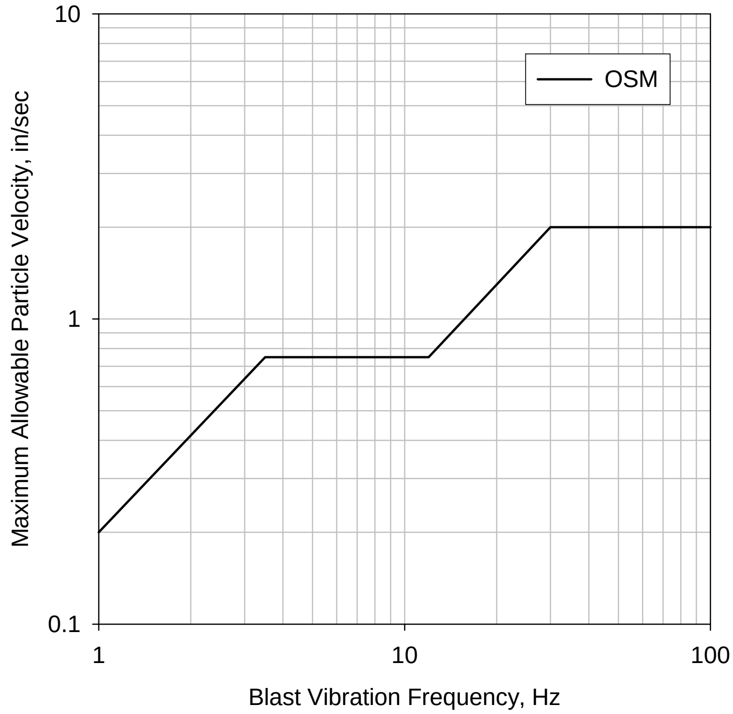

Figure 2-3. Office of Surface Mines blasting level criteria

2.3.1.2 British Standard 7385

In the United Kingdom (UK), British Standard (BS) 7385 considers two types of buildings: industrial or heavy commercial and residential or light commercial. BS 7385 adopted the 2 in/sec criteria originally recommended by the US Bureau of Mines for heavy construction, and adopted a standard slightly more conservative than the OSM criteria for light construction (Figure 2-4). As is the case for the OSM standard, BS 7385 is intended to result in a minimal risk of architectural damage in residential and industrial structures.

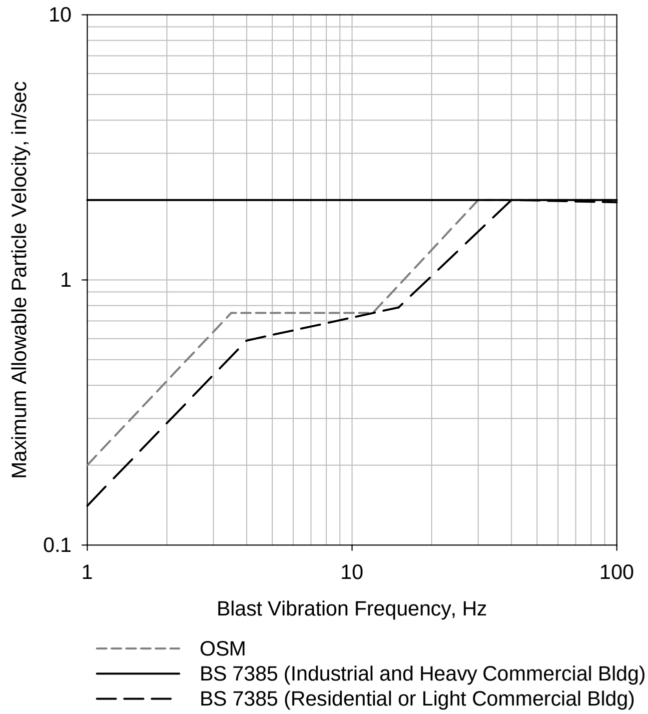

Figure 2-4. BS 7385 compared with the OSM criteria

2.3.1.3 Australian Standard 2187.2

Australian Standard (AS) 2187.2 presents vibration criteria even more conservative than the British standard (Table 2-3).

Table 2-3. Recommended PPV, AS 2187.2 Use of Explosives

Type of Building or Structure	**PPV, in/sec**
Houses and low-rise residential buildings; commercial buildings not included below	0.39
Commercial and industrial buildings or structures of reinforced concrete or steel construction	1 in/sec

2.3.1.4 German DIN 4150 Standard

The German DIN 4150 Standard is based upon human annoyance criteria rather than upon building damage. Because of this difference, the criteria have different applications. The DIN 4150 Standard is shown plotted with the OSM standard in Figure 2-5. The German standard recognizes that that people are more willing to tolerate vibrations in the work place than in their residences.

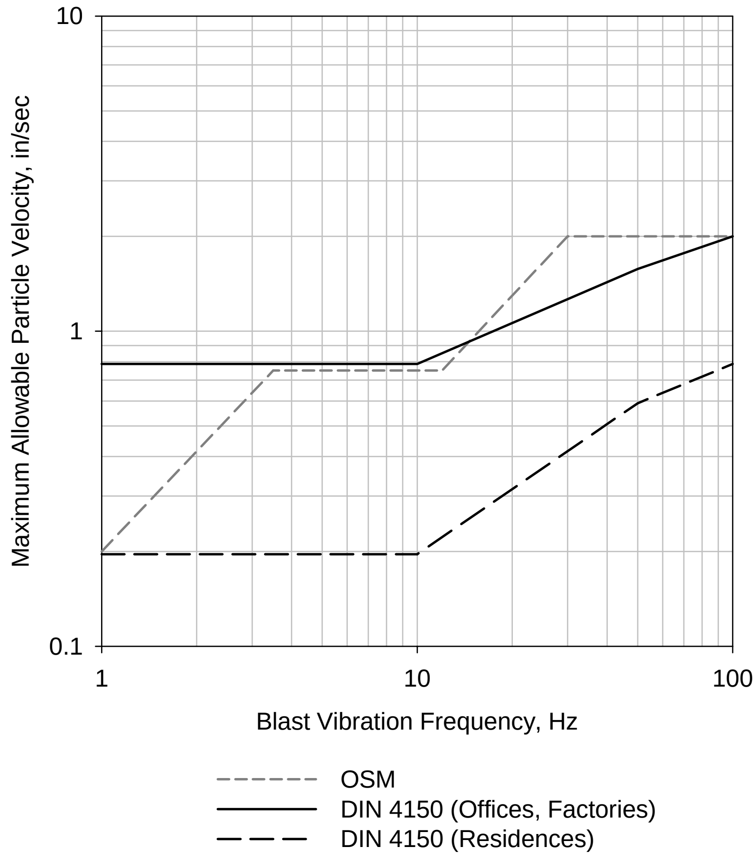

Figure 2-5. DIN 4160 compared with OSM criteria

2.3.2 Continuous Vibration Criteria

Vibrations from highway traffic, trains, and most construction operations (with the exception of blasting and pile driving) are considered to be continuous vibrations. Safe levels for continuous vibration are not well defined (Hendriks 2002). However, a few criteria have been published in the literature.

2.3.2.1 Transport and Road Research Laboratory (TRRL)

The TRRL in the UK has researched continuous vibrations, and proposed the summary of continuous vibration levels and the reaction of people and effects on buildings as presented in Table 2-4.

Table 2-4. Reaction of people and damage to buildings from continuous vibrations (Whiffen and Leonard 1971)

PPV, in/sec	Human Reaction	Effect on Buildings
0.006 - 0.019	Threshold of perception; possibility of intrusion	Unlikely to cause damage of any type
0.08	Readily perceptible	Virtually no risk of “architectural” damage
0.1	Threshold of annoyance	Recommended upper level for “ruins and ancient monuments”
0.20	Annoying to people in buildings	Threshold risk of “architectural” damage to normal dwellings (plastered walls, etc.)
0.4-0.6	Considered unpleasant	Causes “architectural” damage and possible minor structural damage

2.3.2.2 Swiss Standard

The Swiss developed a standard for both transient and continuous vibrations (Table 2-5). The standard takes into account the type of construction, and includes a category for historic items. This standard is very conservative (Henwood and Haramy 2002).

2.3.2.3 FDOT Construction Specifications

Section 455 of the FDOT *Standard Specifications for Road and Bridge Construction* (FDOT 2004), requires vibration monitoring equipment be installed when structure foundations are constructed in close proximity to existing structures. Upon detecting a PPV equal to or greater than 0.5 in/s, the construction operations must be stopped and referred to the Construction Engineer.

Table 2-5. Swiss Standard for Vibration in Buildings (SN 640 312, Swiss Association for Standardization, 1978).

Building Class	Vibration Source	Frequency Range, Hz	PPV, in./sec
I	Machines, traffic	10-30	0.5
		30-60	0.5-0.7
	Blasting	10-60	1.2
		60-90	1.2-1.6
II	Machines, traffic	10-30	0.3
		30-60	0.3-0.5
	Blasting	10-60	0.7
		60-90	0.1-1.0
III	Machines, traffic	10-30	0.2
		30-60	0.2-0.3
	Blasting	10-60	0.54
		60-90	0.5-0.7
IV	Machines, traffic	10-30	0.12
		30-60	0.12-0.2
	Blasting	10-60	0.3
		60-90	0.3-0.5
I – Buildings of steel or reinforced concrete, such as factories, retaining walls, bridges, steel towers, open channels; underground chambers and tunnels with and without concrete lining II – Foundation walls and floors in concrete, walls in concrete or masonry; stone masonry retaining walls; underground chambers and tunnels with masonry linings; conduits in loose material. III – Buildings as previously mentioned but with wooden ceilings and walls in masonry IV – Construction very sensitive to vibration; objects of historical interest			

2.4 HMA Vibratory Compactor Characteristics

Compaction of coarse graded Superpave^{TM} mixtures is sometimes more difficult than with some of the more fine-graded Marshall mixtures (Buchanan and Cooley 2002). While the problem of tender HMA mixes is not new, the adoption of Superpave^{TM} mixtures in general and coarse graded Superpave^{TM} mixtures in particular, has brought attention to the problem of the "tender zone" (Wolters 1998). The tender zone generally occurs within a range of mat temperatures from about 245 to 180° F. Vibratory compaction in the tender zone does not result in any significant additional density of the mat. Because vibratory rollers compact by rearrangement of particles, horizontal movement of the mix particles does not allow confinement of the mix under the roller face.

Coarse-graded mixtures are most readily compacted at relatively high temperatures above the tender zone. (Walker et al 1998). Vibrating double-drum rollers must work immediately behind the paver at higher ground speeds. (Wolters 1998, Stewart 2004).

It is generally accepted that the vibratory rollers should operate at a frequency and ground speed to impact the mat 10 to 14 times per foot. Much of the innovations have been focused on increasing vibration frequency so that compactors can be used to compact HMA mats at higher speeds. Integrating ground speed and vibration control has become a common feature of modern compaction equipment. Vibration amplitude, or vertical distance the drum travels, is also critical. The most effective combination of frequency and amplitude is different for different mixes and lift thicknesses (Stewart 2004).

Table 2-6 contains a listing of some of the currently available heavy vibratory drum rollers available today along with the manufacturer's specification for the equipment. The equipment models listed in the table are regularly discontinued, replaced, or improved. For the latest information on a specific model, the reader is directed to each manufacturer's web site, where the latest information can be obtained.

2.5 Intelligent Compaction

A number of manufacturers are developing what has come to be referred to as intelligent compaction systems. The vision for an intelligent compaction is a system that measures the asphalt stiffness, displays the measurements to the compactor operator, records and maps the stiffness results, and controls the roller compactive effort in response to the measurement system (Caterpillar 2005, Moore 2006). This is achieved by using a measurement and control system to control vibration amplitude, vibration frequency, direction, and ground speed to remediate weak spots and avoid overcompaction (Briaud and Seo 2003).

Figure 2-6 shows a graphic representation of the manufacturers marketing intelligent compactors for soils, aggregates, and hot mix asphalt as of 2006. Although the details of how each manufacturer accomplishes intelligent compaction are proprietary, a few common features are shown in Figure 2-7. The location of the compactor is determined using global positioning system (GPS) receivers. Most manufacturers use accelerometers to measure the relative motion of the drum with respect to the compactor frame. This movement is subsequently empirically related to the stiffness of the layering being compacted. The resulting measured stiffness is used to automatically control the compactive effort. A number of parameters can be controlled, including the amplitude of the vibration, the frequency of the vibration, the direction of the vibration (vertical, horizontal, or any angle in between), and the ground speed of the compactor (Figure 2-8).

The potential benefits of intelligent compaction include increased productivity, improved compaction quality, and more robust information about the stiffness of the material. Increases in productivity may come about as fewer passes are required to achieve density and compaction of thicker lifts may be possible. The elimination of areas with over-compaction or under-compaction will result in improved compaction quality. Areas of inadequate compaction (due to factors such as soils with moisture contents far from optimum) can be identified and corrected. More complete information about the quality of the compaction may reduce the frequency of density measurements with conventional methods. Continuous measurement of stiffness will also provide data on mechanistic properties of materials permitting links between design, construction, and performance (Moore 2006).

The benefits of intelligent compaction in HMA are not universally accepted. Some raise questions concerning the ability of the compactor to distinguish the stiffness of the mat being compacted from stiff layers lying underneath. Some argue that the increase in stiffness in hot mix asphalt may be due to cooling of the mat rather than achieving increased density. Also, some critics are skeptical of the stability of the "feedback loop," i.e., that the system may be unable to measure stiffness while the compaction energy is constantly changing.

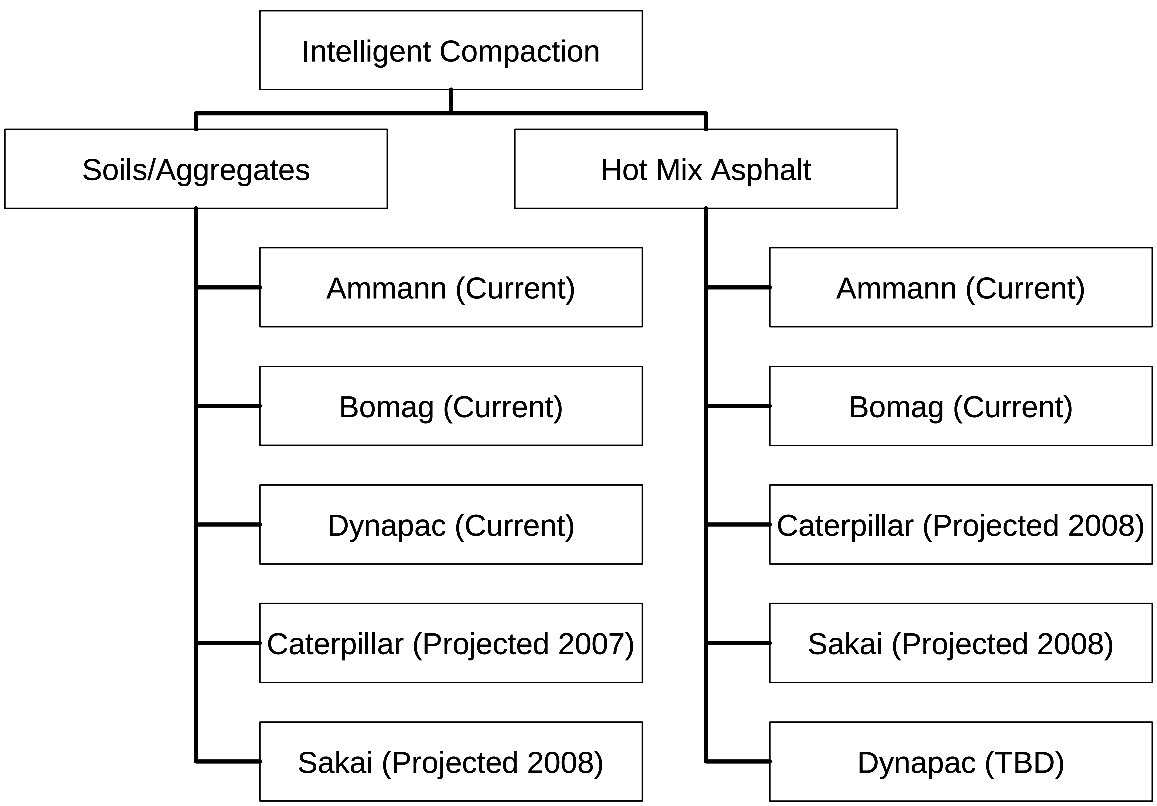

Figure 2-6. Current and projected manufacturers of intelligent compactors as of 2006 (data source: Moore 2006)

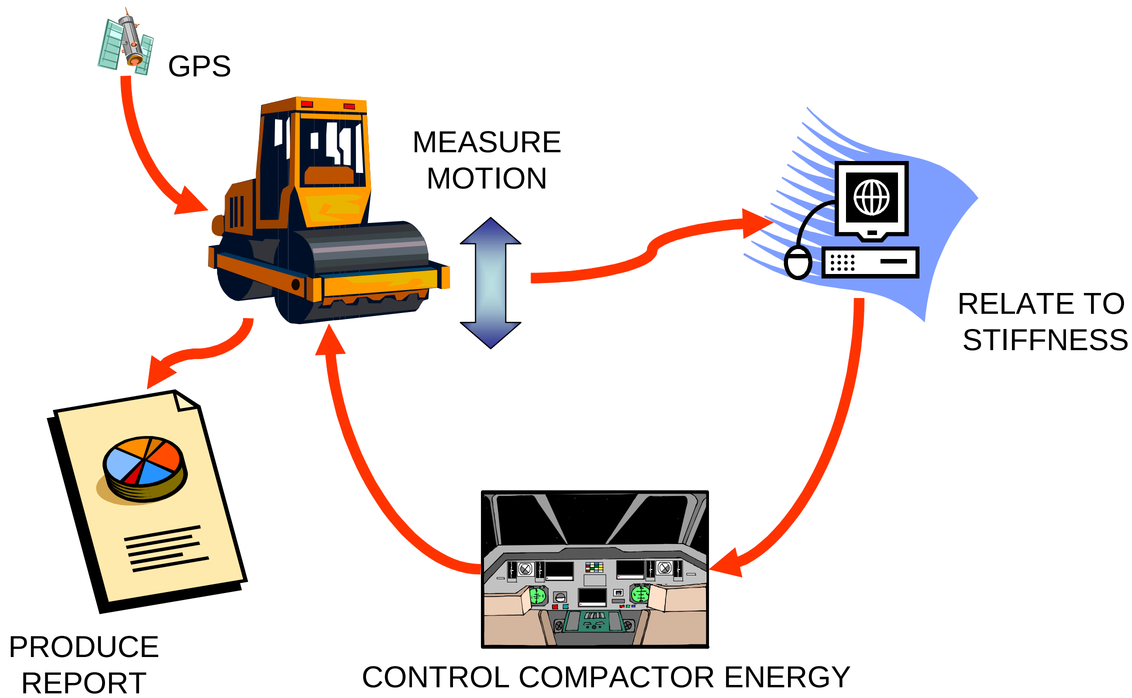

Figure 2-7. Intelligent compaction features

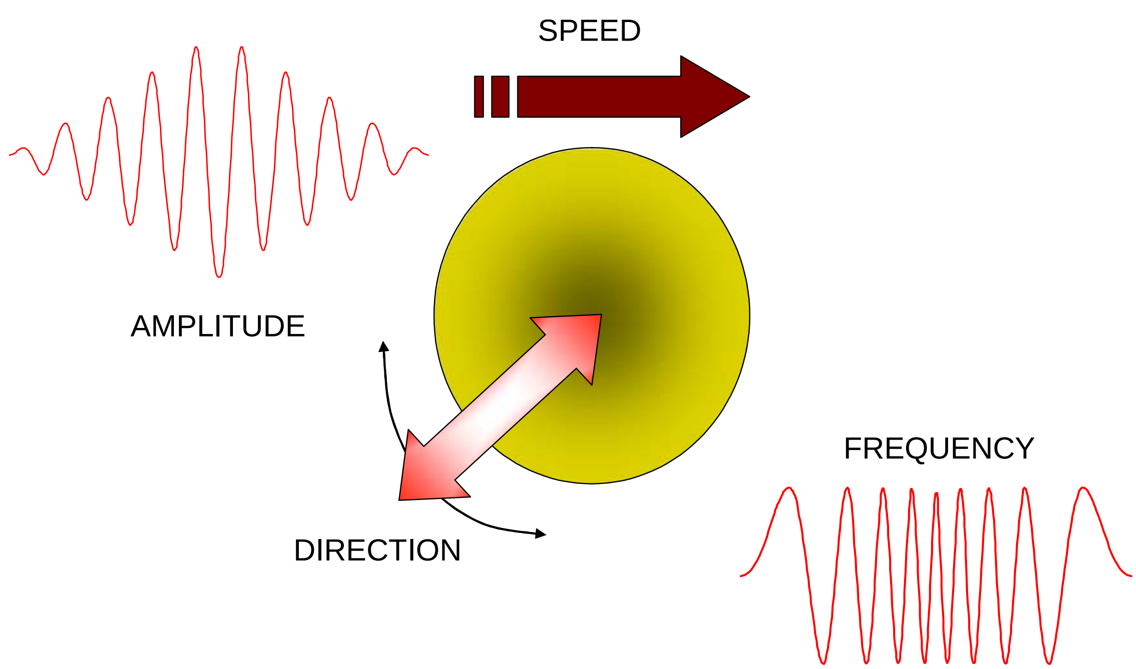

Figure 2-8. Potential vibration parameters adjusted during intelligent compaction

2.5.1 Bomag System

Bomag's HMA compactor intelligent compaction system uses acceleration measurements taken on the vibrating roller drum to measure the contact force between asphalt and roller drum. When calculating the contact force over the vibration path of the drum, each rotation of the eccentric mass produces a loading and unloading curve in which the enveloped area defines the compaction work done (Von Quintus et al. 2004). The dynamic stiffness of the HMA (E_{VIB}) is calculated using the load curve. The cylindrical shape of the drum and the changing contact area of drum and HMA are thereby taken into account. Because HMA stiffness is temperature-related, the surface temperature is measured by an infrared sensing unit underneath the cab and displayed to the operator. Compaction measurements using a nuclear density gauge show a direct correlation between the E_{VIB} vibration modulus and density – given a uniform and stable base under the HMA layer and taking the mat temperature into account. (Von Quintus et al 2004).

The Bomag system uses the measured stiffness values to vary the direction of the compaction energy from fully vertical to fully horizontal (and any angle between) in a process called vectoring. During vectoring, the magnitude of the compactive force is not varied. An on-board microprocessor calculates the mat stiffness and gradually changes the direction of the vibration away from fully vertical toward the horizontal – eventually going to a fully horizontal motion. As the direction of drum motion moves from vertical to horizontal, the compactive effort decreases.

2.5.2 Ammann System

The Ammann intelligent compaction system, called the Ammann Compaction Expert or ACE, uses an electronic measuring and control system to vary the amplitude and frequency of the vibration while indicating the optimum roller speed to the operator. The control algorithm is based upon dynamically measuring the mat bearing capacity up to 50 times per second. The control system reduces the compaction energy as the bearing capacity increases. In the case of HMA, this bearing capacity is directly related to the degree of compaction of the mat using a non-linear correlation between ground bearing capacity and compaction level. Like the Bomag system, the Ammann rollers are fitted with a temperature sensor to measure mat surface temperature. This temperature is used to turn off the vibration if the mat is too hot or too cool for compaction.

Table 2-6. Some current HMA vibratory compactors and their manufacturer's specifications

Model	Operating Mass (lbf)	Drum Width (in)	Drum Diameter (in.	Vibration Frequency Range (Hz)	Nominal Amplitude (in)	Centrifugal Force Range (lbf)
Ammann AV95E	19,200	63	47	35-50	0.012-0.025	11,690
Ammann AV95K	19,400	63	47	35-50	0.012-0.025	11,690
Ammann AV95N	20,900	63	47	25-50	0.012-0.025	11,690
Dynapac CC322	18,300	66	44	51	0.012-0.028	10,390-25,280
Hamm HD 90 HV	20,100	66	48	42-53	N/A	14,850-17,100
Hamm HD O90 H	20,172	66	48	42-50	N/A	11,925-17,100
Bomag BW266	20,600	66	48	57-63	0.020-0.030	27,580-32,950
Hypac C766C	20,600	66	48	33-57	0.020-0.030	17,950-26,375
Ingersoll-Rand DD-90F	21,705	66	48	48-63	0.019-0.025	12,340-38,340
Bomag BW161AD-4 HF	21,826	66	48	45-60	0.016-0.036	27,225-36,000
Terex TV-1700	22,047	66	48	42-50	0.016-0.024	20,475-21,150
Hamm HD 110 HV	22,707	66	48	42-67	N/A	27,675-28,000
Dynapac CC422	22,930	66	51	51	0.016-0.031	15,700-30,960
Dynapac CC422HF	22,930	66	51	50-63	0.012-0.028	16,630-26,070
Caterpillar CB-534D Versa Vibe	22,050	67	51	42-63	0.013-0.041	18,570-22,234
Sakai SW800	22,930	67	51	42-67	0.013-0.022	10,580-27,120
Dynapac CC522	26,130	77	55	51	0.012-0.028	15,700-30,960
Dynapac CC522HF	26,130	77	55	50-63	0.008-0.024	16,630-26,070
Bomag BW278	23,500	78	48	57-63	0.020-0.030	30,368-37,099
Hypac C778B	23,500	78	48	33-53	0.020-0.030	22,375-31,150
Ingersoll-Rand DD-112F	25,360	78	55	50-70	0.133-0.032	33,090-42,070
Hamm HD 120 HV	27,675	78	55	42-50	N/A	29,025-38.700
Caterpillar CB-534D XW Versa Vibe	24,917	79	51	42-63	0.010-0.034	18,570-22,234
Ingersoll-Rand DD-118HFA	27,260	79	55	50-70	0.013-0.032	33,090-42,070
Sakai SW850	27,560	79	55	42-67	0.013-0.022	13,070-33290
Dynapac CC622HF	27,785	84	55	51-64	0.008-0.024	17,310-31,025
Bomag BW284	28,425	84	54	60-67	0.016-0.026	34,665-41,235
Hypac C784	28,425	84	54	57-67	0.016-0.026	34,665-41,235
Sakai SW900	28,660	84	55	42-67	0.014-0.024	15,210-38,800
Ingersoll-Rand DD-138HFA	30,325	84	55	45-67	0.014-0.036	36,685-41,715
Hamm HD 130 HV	30,430	84	55	42-53	N/A	35,100-43,650
Ingersoll-Rand DD-158HFA	33,810	84	59	42-57	0.017-0.035	37,170-44,120

3 ANALYTICAL MODEL DEVELOPMENT

3.1 Hypotheses

The following hypotheses were evaluated using an analytical model validated by field data analysis.

- Most of the energy from the FWD and vibratory roller is contained in Raleigh waves. Raleigh waves diverge from their source as cylindrical waves, a two dimensional phenomenon. Therefore, we can scale the range from the source (FWD or vibratory compactor) using square root scaling; i.e., the scaling factor will be equal to the inverse of the square root of the energy.

- From the FWD data, we can characterize a site by developing a plot of peak velocity versus scaled range. This plot will serve as an upper bound predictor of ground motion.

3.2 Scaling of ground motion

Scaling or normalizing of ground motion is based on the geometric dispersion of the ground motion induced by a dynamic source. For explosive sources, the motion propagates from a spherical source. Ground motions are generated by the spherically divergent energy, and hence the energy per unit volume decreases at the same rate as the volume increases. The volume of a sphere is directly proportional to the cube of its radius, r. In a perfectly elastic media, the only decay of motion is due to the geometric divergence of the source energy or simply $1/r^3$. If the explosive has a weight of w pounds we can relate that to the energy of the source by the physics of thermodynamic of explosives. Range, R, is usually scaled or normalized using the weight, since there is a direct relationship between an explosive’s mass and energy. Scaled range then is $R/w^{1/3}$. More correctly stated this scaling is represented by $R/U^{1/3}$, where U is the energy of the source. This procedure works quite well even for surface waves, because they are generated by the spherically divergent air blast wave.

For the loading of an FWD or vibratory compactor there is no air blast or spherically divergent wave. Approximately 80% of the ground motion energy goes to producing Raleigh and shear waves, and this energy propagates as a cylindrical wave. Thus, the energy per unit volume that generates the surface waves is decreasing proportionally with the volume of a cylinder. The volume of a cylinder is proportional to r^2, and hence the perfect decay would be $1/r^2$. The scaling law becomes $R/U^{1/2}$. In the scaling of the data from the FWD and the vibratory compactor we have chosen to use this more exact form for scaling since our sources are similar, and the energy scaling parameter is the unknown that we are trying to determine.

It should be noted that none of these scaling laws are perfect in the real world. For example, if data from the FWD were collected in the pavement beneath and close to the loading plate, the divergence would be primarily spherical, since the ground motion in this region is a dominated by a compressive wave. In fact as we move the data collection into regions very close to the vibratory compactor, the wave may also appear spherically divergent. The basic idea in scaling is to remove the effect of the source geometric divergence from the data analysis. When ground motion data is plotted in this scaled fashion, the decrease in amplitude with scaled range is the loss due to the media that the wave is traveling through.

Scaling of the FWD is a straight forward procedure. The input energy is easily computed knowing the peak input force, F, and the maximum displacement, d_0, generated at the input. The energy is then, $U=F \times d_0$ and the scaling parameter is $1/U^{1/2}$. Our challenge was to determine the energy input from the vibratory roller. In a perfect world one impact from the vibratory roller and its associated energy would be sufficient. This would be equivalent in the explosive world of knowing the weight of the charge. But we have surface waves that are generated by the moving vibrator, and these waves must travel through a layered media and stabilize into a standing wave. Stabilization occurs when all of the constructive and destructive interference has settled out. This also includes the filtering action of the layered system, i.e. frequency shift and phase shifts.

3.3 Finite Element Code Description

A finite element code based upon the program developed by Dr. S. W. Key at Sandia National Laboratories was adopted as the analytical model for this project. The code is designed to compute time-dependent displacements, velocities, accelerations, and stresses within elastic or inelastic, two-dimensional or axisymetric solids of arbitrary shapes and materials. The code solves the equations of motion at each time step for a series of lumped masses that are formed by distributing each element’s mass to the node points that define the element. Time integration for node point velocities and displacements are carried out using a central difference method integration scheme. This integration scheme is conditionally stable with respect to time step size.

The code uses first-order, isoparametric, quadrilateral finite elements as well as the usual finite element techniques for calculating both element strains from nodal displacements and nodal loads from uniform element stresses.

To apply the FE method we first discretize the continuum with an overlay of a Lagrangian grid. The mass of the media is lumped at the nodes by a volumetric distribution. The mass points are connected with “springs” that have stiffness properties of the continuum connecting them. We derive this connection by making assumptions of the form of the displacements (axisymmetric, plane strain, etc.) in the continuum and hence the strain distribution. The resulting equilibrium forces are arrived at by applying minimum energy principles. The resulting constraints, such as the nodes are connected by straight lines, yield a stiffness matrix. This matrix becomes our “springs,” and now we have a series of masses connected by springs much like a bed spring system with masses at the spring connections.

The resulting equations are a system of coupled ordinary differential equations relating the external forces to the nodal displacements by a stiffness matrix. For dynamics problems, the system of equations also contains inertial terms and possibly damping terms. By D'Alembert these terms are just added to the static resisting force, and the resisting force is set equal to the external forces.

This system of equations is "locally" integrated by stepping the load forward in time and using the central difference finite difference formulation to solve for the nodal accelerations, velocities and the displacements. The global stiffness matrix is never formed; hence this is a local equilibrium solution. This technique works very well for highly inertia sensitive problems such as traveling waves. There is one draw back in that the scheme is only conditionally stable. The time step must be chosen based on the Courant stability criteria or smaller to maintain a stable solution during the time of interest.

Once the displacements are known for the time step, the strains are evaluated at the center of the element using the same formulation as in deriving the stiffness matrix. With the strains known the stresses are evaluated using the constitutive law for the element material. These stresses are then distributed to the nodes and converted to the internal forces of the system. To maintain stability "artificial viscosity" forces are added to these forces. The formulation of these artificial forces is the same that is used for the central finite difference schemes used to directly integrate the potential functions when the finite element formulation is not used. That is to say, we write the entire system of field equations for the continuum problem at hand and then transform them into a discrete finite difference form. This discrete form is in space and time with some very restrictive conditions on the boundaries and the shapes of the continuum discretization.

Finally the external forces are stepped forward as previously mentioned; the internal forces are subtracted with the resulting out of balance forces causing motion. The scheme starts all over again by solving for the accelerations, velocities, and the displacements.

3.4 Field Testing

3.4.1 Site Description

A field test was performed to explore the relationship between FWD data and vibratory compaction during construction. Data were acquired during vibratory compaction of the structural HMA layer on SR 207 (State Project No. 78050-3531) in St. Johns County near St. Augustine, Florida, (Figure 3-1).

.

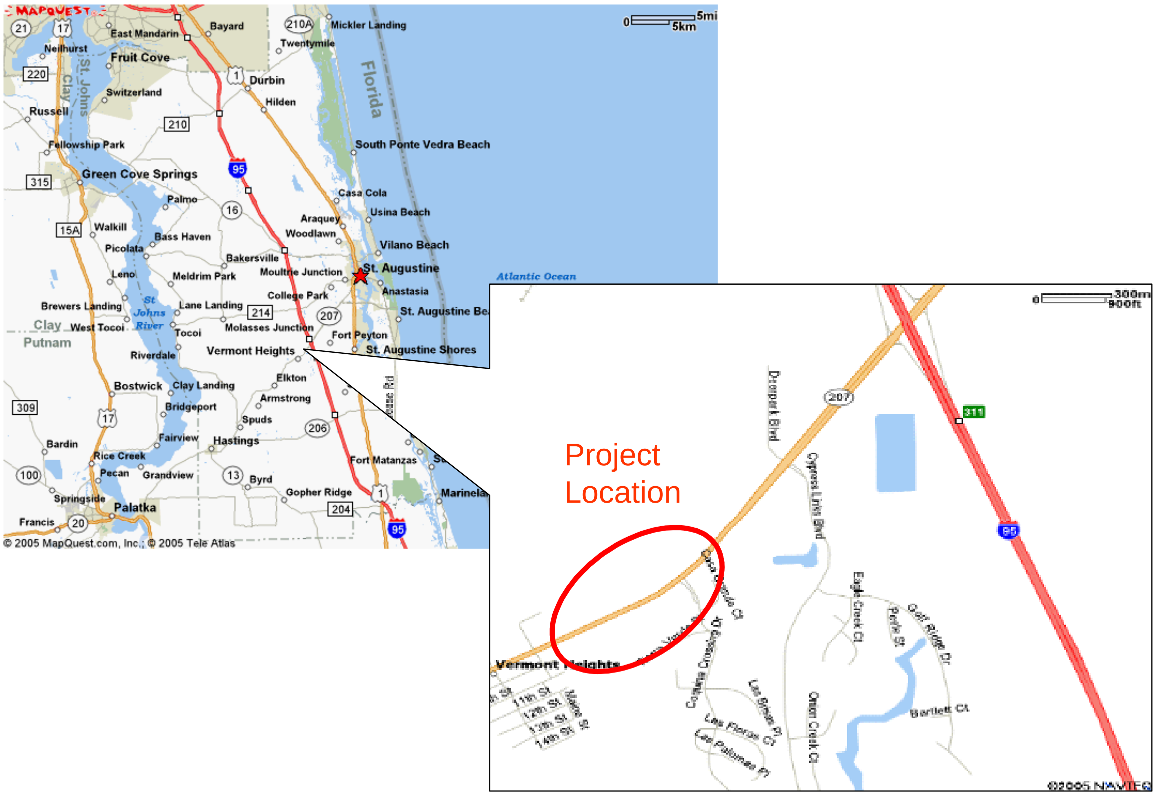

Figure 3-1. Location of field testing on SR 207

The pavement structure consisted of 4 inches of HMA, 12 inches of limerock base, and 12 inches of stabilized subgrade over a sandy subgrade (A-3 and A-2-4) with no bedrock near the surface. The ground water table was estimated at four feet below the surface.

An Ingersoll-Rand (IR) DD-110 HF Vibratory asphalt compactor was used for compaction. The compactor was operated at a vibration frequency of 42 Hz and vibration amplitude of 0.022 in.

3.4.2 Data Collection

Far field ground motions were recorded on October 19, 2005, at two locations as shown in Figure 3-2 by FDOT personnel using the Instantel MiniMate Plus™ data acquisition units (Figure 3-3). This instrument features triaxial geophones for measuring particle velocity in three orthogonal directions (longitudinal, transverse, and vertical). Two data acquisition units were employed at the site: unit 5401 was used to record the ground motion at 17 feet from the centerline of the paving lane, and unit 5532 was used at 27 feet from the centerline of paving lane. The instruments were set to record the full waveform time histories.

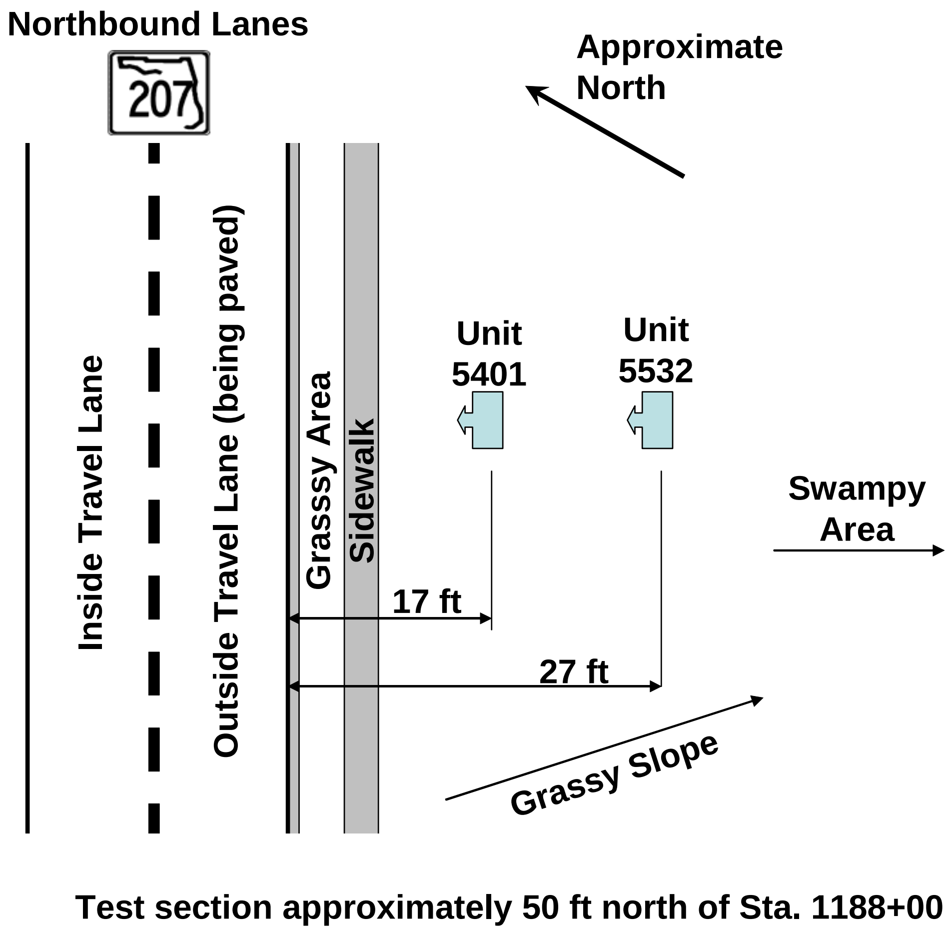

Figure 3-2. Approximate locations of data acquisition units with respect to roadway

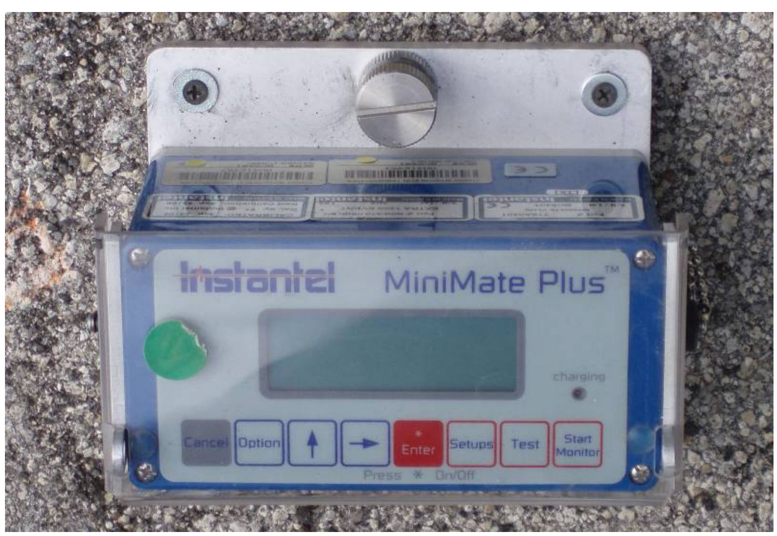

Figure 3-3. Photograph of data acquisition unit

3.4.3 Field Measurement Results

Table 3-1 presents a summary of the SR 207 tests results. Here, the results are presented in terms of the PPV in each of the longitudinal, transverse, and vertical directions, along with the peak vector sum. The dominant frequencies in longitudinal, vertical and transverse directions are also presented.

Table 3-1. Summary of results from SR 207

Unit 5401 (range = 17 feet from center of travel lane)								
		PPV, in/sec				Dominant Frequency, Hz		
Travel Direction	Trigger Time	Longi-tudinal	Vertical	Transverse	Peak Vector Sum	Longi-tudinal	Vertical	Transverse
South	12:53:02 PM	0.331	1.180	0.481	1.116	32.5	33.0	33.0
North	12:56:25 PM	0.333	1.100	0.562	1.150	33.1	33.1	33.1
South	1:06:42 PM	0.411	1.180	0.517	1.230	32.9	33.5	32.9
Avg.		0.358	1.153	0.520	1.165	32.8	33.2	33.0
Unit 5532 (range = 27 feet from center of travel lane)								
		PPV, in/sec				Dominant Frequency, Hz		
Travel Direction	Trigger Time	Longi-tudinal	Vertical	Transverse	Peak Vector Sum	Longi-tudinal	Vertical	Transverse
South	12:53:03 PM	0.216	0.494	0.365	0.577	49.5	33.1	32.5
North	12:56:26 PM	0.342	0.549	0.343	0.618	33.0	32.8	66.3
South	1:06:45 PM	0.226	0.512	0.369	0.564	49.5	32.9	32.9
Avg.		0.261	0.518	0.359	0.586	44.0	32.9	43.9

As previously mentioned, the data acquisition units were programmed to capture full waveform time histories. Figure 3-4 shows a typical waveform history of vertical particle velocity. A fast Fourier transform (FFT) was performed on the time history data to obtain the frequency spectrum shown in Figure 3-5 indicating a dominant frequency of approximately 34 Hz with harmonics occurring at approximately 48 and 66 Hz. In Figure 3-6, a typical particle trajectory is plotted. The data trace has the characteristic retrograde motion expected from Raleigh waves and confirms the hypothesis that the majority of the ground motion energy is contained in the Raleigh waves.

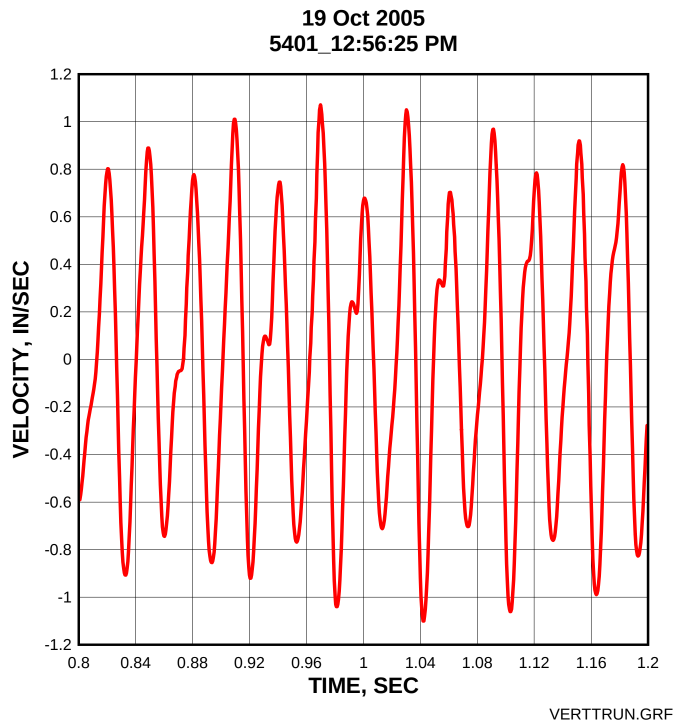

Figure 3-4. Typical vertical particle velocity time history at a range of 17 ft

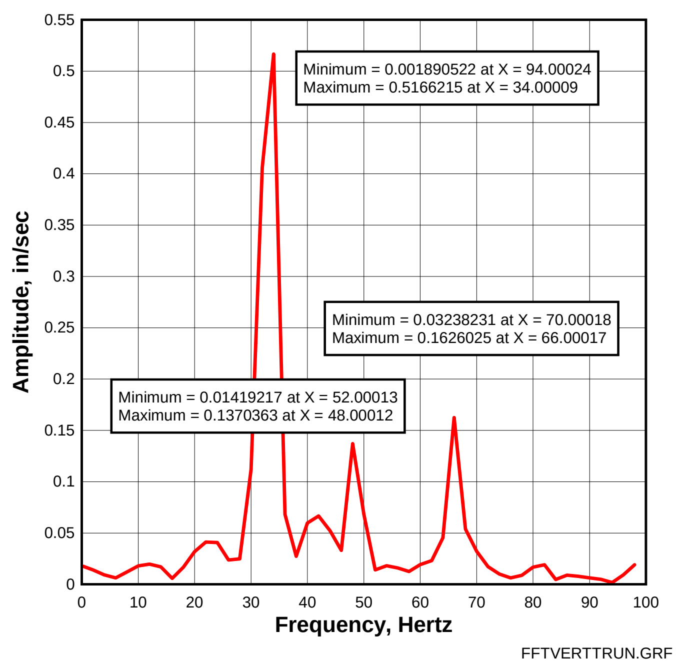

Figure 3-5. Typical FFT frequency spectrum at a range of 17 ft

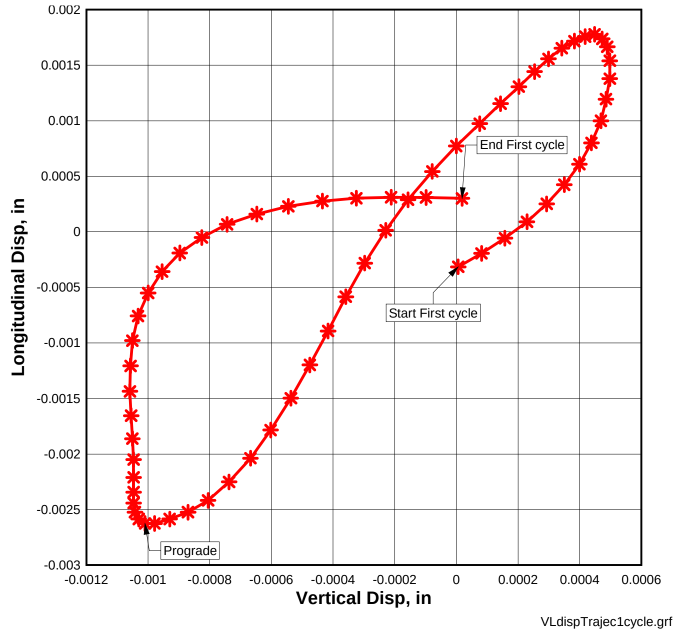

Figure 3-6. Typical particle trajectory, SR 207

3.5 Calculations

Finite element calculations were performed on the pavement section shown in Figure 3-7 to directly compare the model with data from the field. This calculation was run as a plane strain problem. The boundary at the loaded elements is a force input to the nodes. The horizontal extent of the grid (100 ft) was chosen far enough away to eliminate reflections from returning during the time of interest. The right-hand boundary was restricted to vertical motion with the radial motion fixed to zero displacement. The bottom of the grid was restricted to radial motion with the vertical motion fixed to zero. Several computations were performed with this boundary at different depths to test the effect of the interference of the reflections in the surface waves of interest. There was little effect since the Raleigh wave is a shallow (in depth) phenomena. The bottom was set at about the water table level. These bottom reflections approximate the reflections that would occur from the saturated soil at the water table.

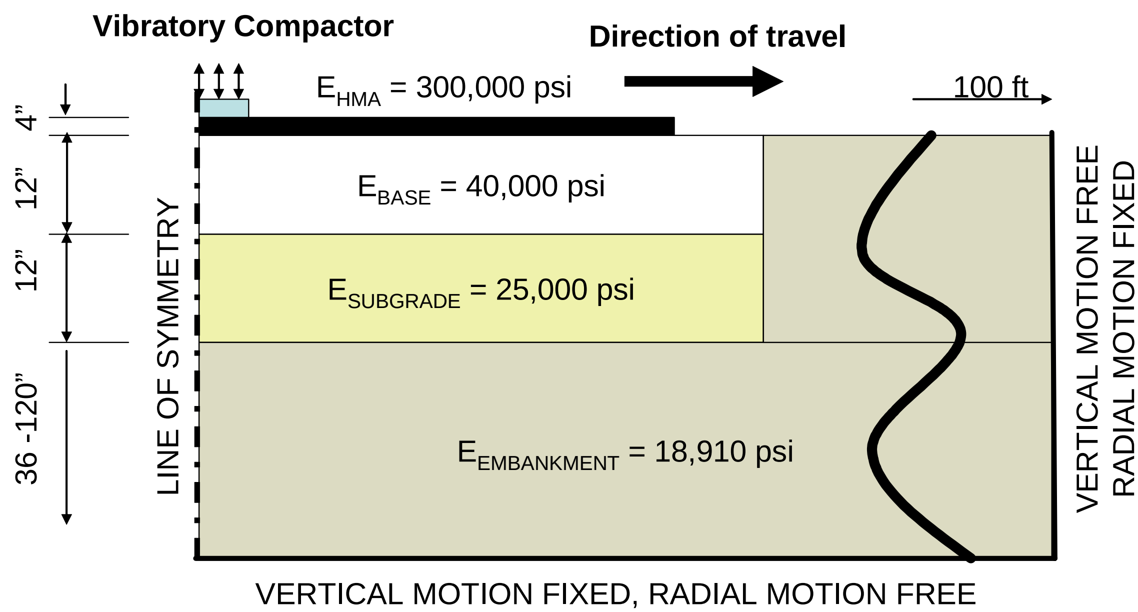

Figure 3-7. Plane strain model idealization for vibratory roller calculations

The boundary between the various layers was fixed, i.e., there was compatibility of displacement at the interface, thus no slippage of one material past another was allowed.

Some results from the model are presented in Figure 3-8. On the right is a frequency spectrum from the model at a range of 27 ft, while the left plot shows field data at the same range. This indicates that the model accurately predicts the predominant frequency and, to a lesser extent, the harmonic frequencies characteristic of the field data. This indicates that the model adequate replicates the wave propagation in the system and that all boundary conditions are properly modeled to capture the essential features of the ground motion over the necessary time period.

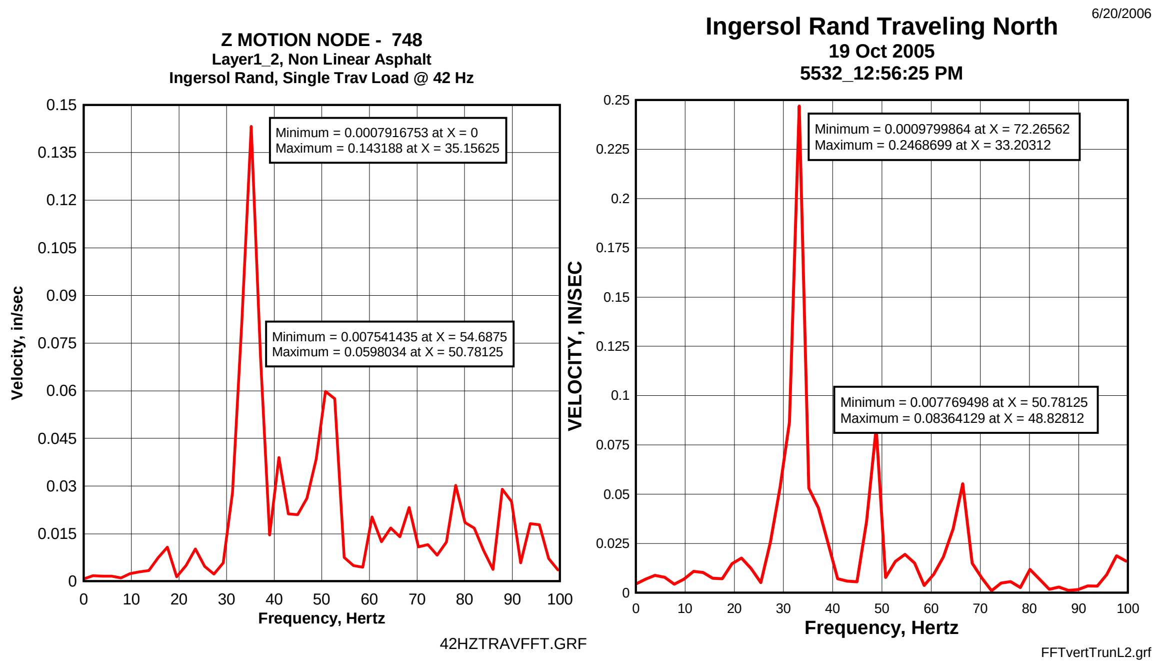

Figure 3-8. Frequency spectrum comparison of model (right) and field data (left).

No FWD time histories were available for the SR 207 site; therefore, it was necessary to develop a finite element model of the site, load it with a typical FWD load-time history, and calculate the resulting velocity-time histories. An axisymmetric model was chosen as shown in Figure 3-9. The left-hand boundary is the line of symmetry for the axisymmetric FWD calculations. It is restricted to motion only in the vertical direction. The radial motion is restricted to zero displacement. The right-hand boundary was restricted to vertical motion with the radial motion fixed to zero displacement. The bottom of the grid was restricted to radial motion with the vertical motion fixed to zero. The bottom was set at about the water table level depth.

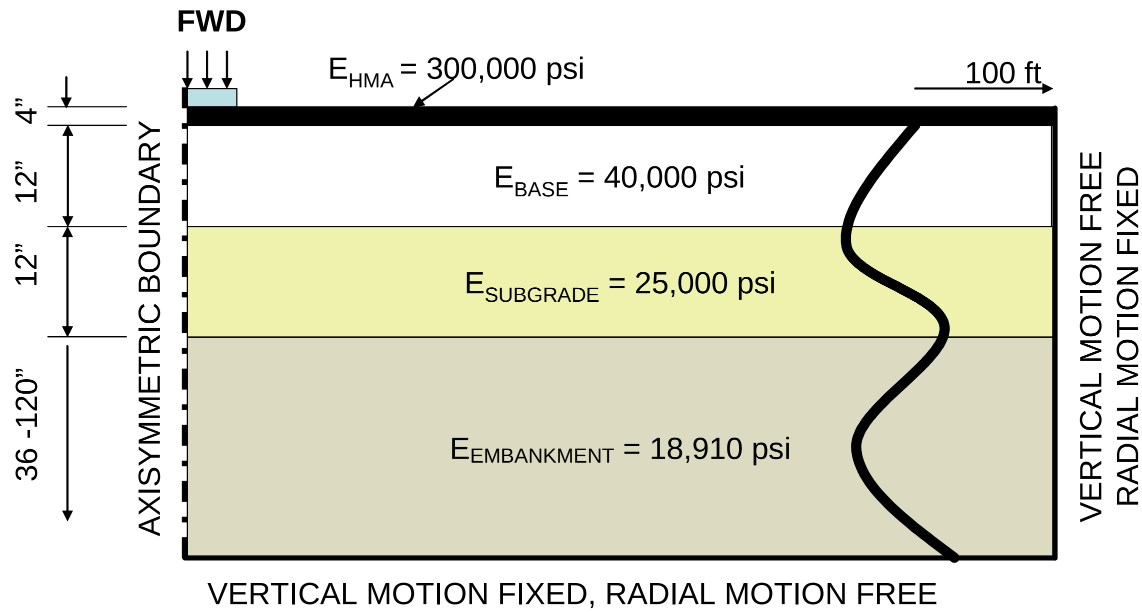

Figure 3-9. Model idealization for FWD calculation

Figure 3-10 shows the nominal energy time-history from a simulated FWD drop. The peak energy is approximately 13 ft-lbs at approximately 16 msec.

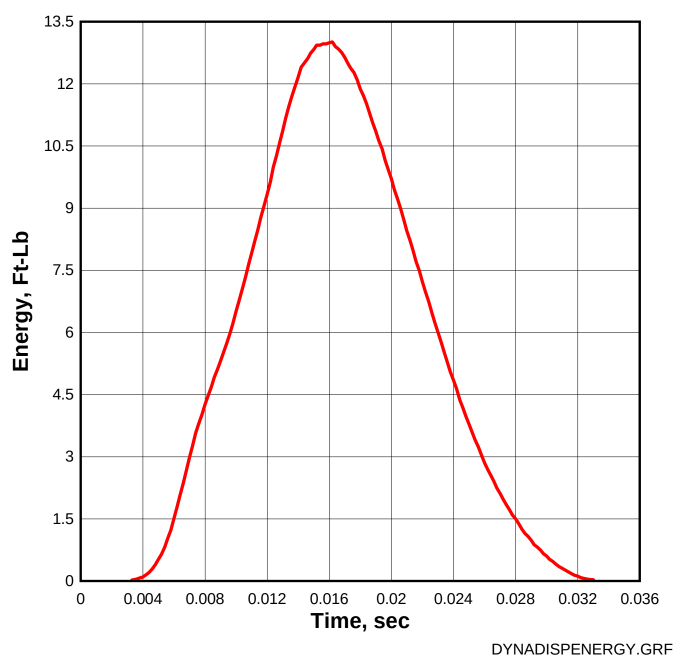

Figure 3-10. Nominal FWD energy

The results of the calculations for both the FWD and the vibratory roller are plotted in Figure 3-11. This plot illustrates the need to use scaling to directly compare the two energy sources. Recall that Raleigh waves diverge from their source in a cylindrical fashion, and a square root scaling law should apply. In Figure 3-12, the ranges from each source have been scaled by dividing the range in ft by the square root of the peak energy input of the source. It can be seen from the figure that using square root scale causes these two curves to overlay one another. This confirms the hypothesis that the range can be scaled using square root scaling.

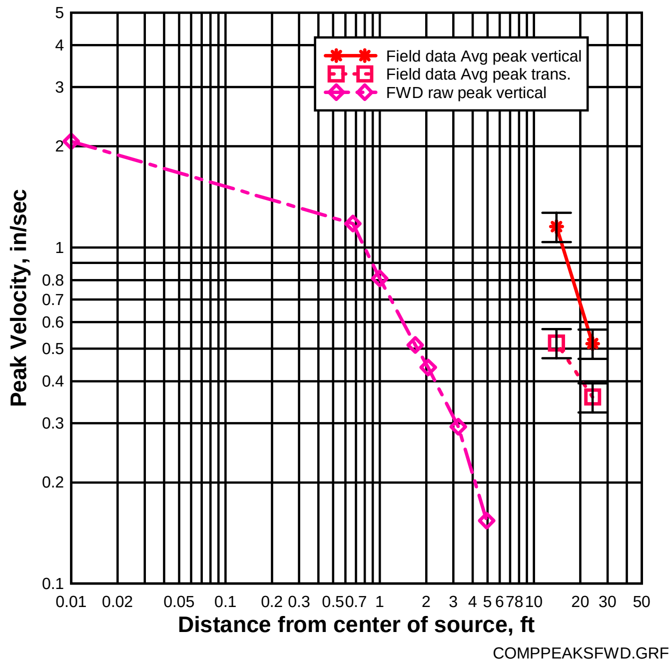

Figure 3-11. Un-scaled peak velocity versus range

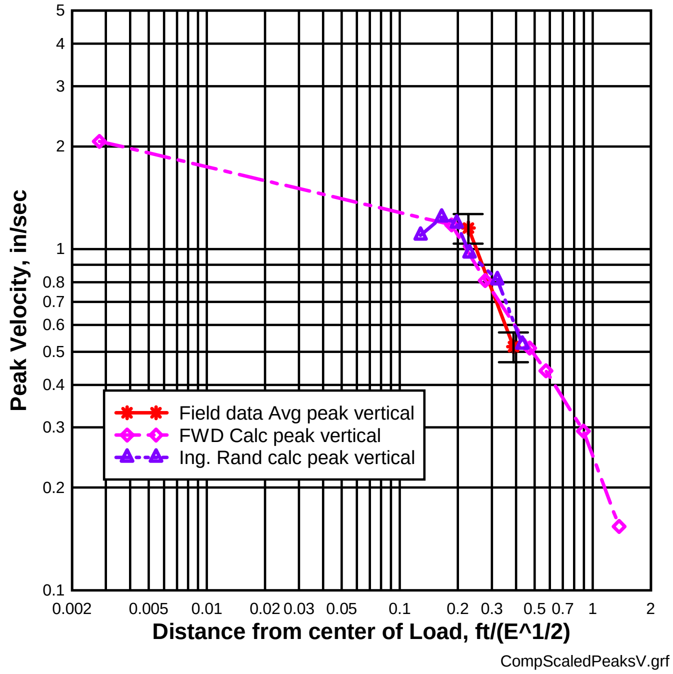

Figure 3-12. Peak velocity versus scaled range

4 VIBRATION CHARACTERIZATION

4.1 Procedure

4.1.1 Criteria

As described in Chapter 2, various Federal, State, and foreign agencies have proposed vibration limit criteria, some intended to mitigate damage to structures, while others are based upon limiting human annoyance. We have selected two of these criteria to form the basis of our recommendations. Figure 4-1 is a log-log plot of peak particle velocity versus roller frequency. The plot has been divided into three zones:

- The RED ZONE designates a region of the plot were damage to structures is possible.
- The YELLOW ZONE designates a region of the plot where human annoyance is possible, but damage to buildings is unlikely.
- The GREEN ZONE designates the region of the plot were ground motions may or may not be noticeable by persons, but human annoyance is unlikely.

The boundary between the RED and YELLOW ZONES follows the criteria of the U.S. Office of Surface Mining (OSM), the most often cited empirical vibration damage criteria for residential construction. The boundary between the GREEN and YELLOW ZONES follows the German DIN 4150 Standard based upon human annoyance criteria in residences. Both of these criteria are considered by the research team to be trustworthy and not unnecessarily conservative.

Conditions in the RED ZONE should be avoided to prevent possible architectural or structural damage to buildings. Conditions in the YELLOW ZONE are acceptable; however, the department should be prepared to receive and answer complaints from building occupants who may be annoyed by the vibration. Operations in the GREEN ZONE should incur few, if any, complaints from the public.

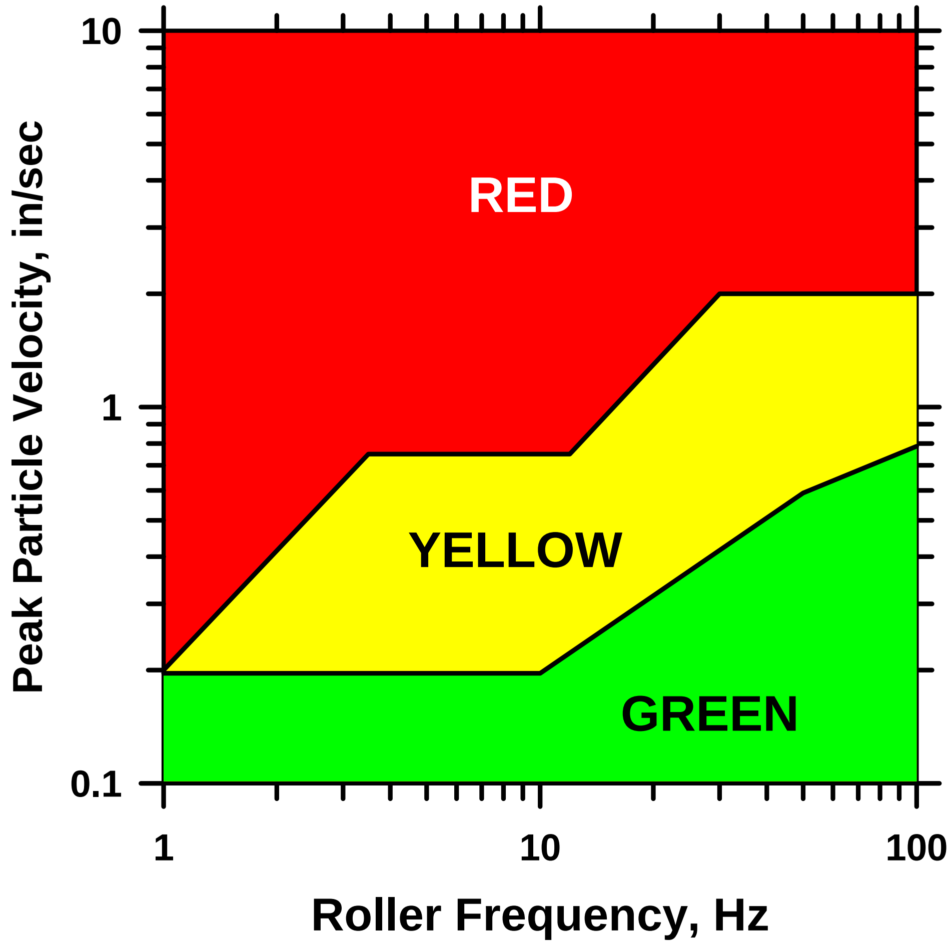

Figure 4-1. Recommended vibration criteria

Recall that the objective is to use FWD data at a site to develop a predictor that will isolate cases where ground motions from a vibratory compactor could cause structural damage. The analytical study described in Chapter 3 demonstrated that scaled range can be calculated using a square root scaling law and that FWD data can be used to characterize a site by developing a plot of peak velocity versus scaled range. This plot serves as an upper bound predictor of ground motion. Detailed knowledge of the pavement layers and site geology is not required.

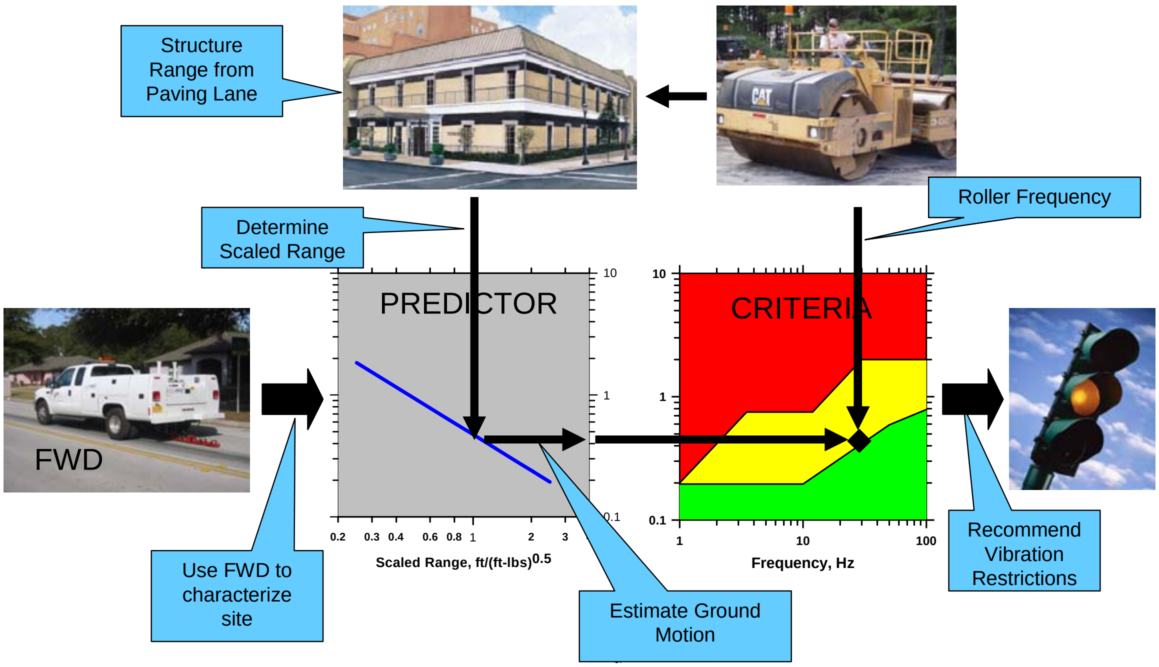

Figure 4-2. Diagram illustrating procedure

4.1.2 Site Characterization

The first step is to develop the curve that will serve as the predictor of ground motion. This is accomplished using FWD data, specifically the time histories of the recorded motions. All FWDs have the capability to record the full displacement time histories; however, this is usually not done because they are not used for production calculations. The FWD geophone sensors measure velocity time histories. The velocity data are subsequently filtered and numerically integrated in the FWD data acquisition computer to obtain displacement time histories. The peak values of displacement at each sensor are observed and recorded to form the deflection basin commonly used for FWD forward and back calculation procedures.

At the request of District engineers, the State Materials Office (SMO) routinely performs FWD testing to evaluate embankment stiffness. In order to properly assess the roadway and coordinate maintenance of traffic (MOT), the SMO requires the requesting engineer provide certain project information. Future flexible rehabilitation projects within urban areas or near vibration sensitive structures should be identified by the Engineer before the SMO is requested to perform deflection testing.

Typically, project information required by the SMO includes:

- Roadway ID
    - State Road Number
    - Financial Project ID
    - County Section Number
- County name

- Project limits
- Project map
- Number and direction of roadway lanes
- Identification as a potential vibration-sensitive project
- Exceptional needs
- Night-time testing
- Shoulder testing
- Recommended due date

When the requesting Engineer identifies the project as potentially vibration-sensitive, the SMO should record the full FWD displacement time histories for each production drop.

4.1.3 Calculations Required

4.1.3.1 Ground Motion Predictor Curve

The first step is to develop a project-specific ground motion predictor curve from the FWD time histories. This plot will serve as an upper bound of expected peak particle velocity as a function of scaled range. It is developed from the measured displacement time histories from the FWD. Because the Raleigh wave does not fully form until some finite distance from the impact source, the displacement-time history at the center of the FWD load plate is not used in the analysis.

It is necessary to develop the particle velocity time histories, *v(t)*, from the FWD displacement time histories, *x(t)*. This is straight forward by means of differentiation of the displacement time history:

$$v\ (t) = \frac{d}{dt} x(t) \qquad \text{(Equation 4-1)}$$

This derivative can be readily approximated by simple numerical differentiation using the central difference formula:

$$v_i = \frac{x_{i+1} - x_{i-1}}{t_{i+1} - t_{i-1}} \qquad \text{(Equation 4-2)}$$

where v_i is the velocity at time step i, x_{i+1} is the displacement at time step $i+1$, t_{i+1} is the time at time step $i+1$, etc. Because the displacement time histories have been processed and filtered by the FWD data acquisition software, the numerical differentiation is smooth and easily accomplished. The peak velocities at each sensor are then readily determined:

$$(v)_{\max} = \max_i v_i = (PPV)_{FWD} \qquad \text{(Equation 4-3)}$$

The FWD energy input into the system, W_{FWD}, is calculated at each time step from the FWD force F and displacement z as follows to create an energy time history:

$$(W_{FWD})_i = F_i \times z_i \qquad \text{(Equation 4-4)}$$

The peak energy input by the FWD is easily obtained from this data from the energy time history

$$(W_{FWD})_{\max} = \max_i \left(W_{FWD}\right)_i \qquad \text{(Equation 4-5)}$$

The FWD energy scaling factor is then calculated as

$$SF_{FWD} = \frac{1}{\sqrt{(W_{FWD})_{\max}}} \qquad \text{(Equation 4-6)}$$

The scaled range SR is given by

$$SR = D \times SF_{FWD} \qquad \text{(Equation 4-7)}$$

where D is the distance from the center of the load plate to the FWD transducer. The scaled ranges of the FWD transducers are subsequently plotted versus the peak particle velocity on a log-log plot. The data from all production drops should be plotted excluding the sensor directly under the loading plate. Using non-linear regression, a power curve of the form

$$\left(PPV\right)_{predicted} = b \times (SR)^m \qquad \text{(Equation 4-8)}$$

is fit to the data, where b and m are regression constants. The resulting curve represents the best fit predictor of the peak particle velocity as a function of scaled range. To ensure a conservative prediction of PPV, we calculate the 95% confidence interval on Equation 4-8. The resulting prediction error in Equation 4-8 is given by

$$\varepsilon = \left(PPV\right)_{FWD} - \left(PPV\right)_{predicted} \qquad \text{(Equation 4-9)}$$

These error values are calculated for each FWD drop, and the standard deviation of the error S_ε is calculated. This value is subsequently used in Equation 4-8 to give the final predictive equation of PPV versus scaled range

$$\left(PPV\right)_{predicted} = (b + 1.96 S_\varepsilon) \times \left(SR\right)^m \qquad \text{(Equation 4-10)}$$

4.1.3.2 Vibratory Compactor Peak Energy

We must determine the amount of energy that the vibratory roller will impart to the system so that we can scale the locations (range to nearest traffic lane to be paved) of the structures. Table 4-1 lists the vibratory compactor parameters required in the calculations. These parameters will vary with manufacturer and model, and, if possible, should be specific to the vibratory roller to be used on site. However, in many cases, it may not be possible to know in advance the make and model of the compactor to be used on the site. In this case, default values for these parameters have been listed in Table 4-1. These default parameters are based upon published data for the Ingersoll-Rand DD-158HFA, the largest production HMA vibratory roller on the market at the time of this report. To obtain a conservative estimate of the input energy, the worst case conditions should be employed. To aid the user, Table 4-1 summarizes whether a larger or smaller value of the parameter is a worse condition. The parameters for a particular roller may be obtained from the manufacturer, and are typically found on the manufacturer's web site.

Table 4-1. Vibratory compactor parameters required and default values

Property	Default Value†	Comments
Peak Load, P (lbf)	44,120	Larger is worse condition
Amplitude, A, (inches)	0.035	Larger is worse condition
Frequency, f (Hz)	42	Smaller is worse condition
Drum Diameter, d_{drum} (inches)	59	Larger is worse condition
† Based on Ingersoll-Rand DD-158HFA.		

In order to calculate the energy input of the roller into the system, we must estimate the number of blows over a characteristic length, L. We have chosen to define L in terms of the drum diameter d_{drum} as follows:

$$L = k \times d_{drum} \qquad \text{(Equation 4-11)}$$

where k is an empirical calibration factor. It was our assumption that k = 1 was sufficient.

While the ground speed will vary depending upon the characteristics of the roller and the experience of the operator, most operators will control the speed such that the roller will impart approximately 10 to 14 blows per linear foot of distance traveled. We recommend that an average number of 12 blows per linear foot (or 1 blow per linear inch) be assumed. Thus the total number of blows in the characteristic length can be calculated as

$$N = L \times n = k \times d_{drum} \times n \qquad \text{(Equation 4-12)}$$

where n is the number of blows per inch. The energy input into the system per blow of the roller is given by the product of the peak load, P, and the peak amplitude, A. Therefore, the characteristic energy input of the roller is given by the energy input per blow times the number of blows in the characteristic length:

$$W_{roller} = k \times d_{drum} \times n \times P \times A \qquad \text{(Equation 4-13)}$$

We can then determine the roller scale factor using square root scaling as follows:

$$SF_{roller} = {}^{1}\!/\!\sqrt{W_{roller}} = {}^{1}\!/\!\sqrt{k \times d_{drum} \times n \times P \times A} \qquad \text{(Equation 4-14)}$$

We then scale the range to the critical structure using SF_{roller} and enter the peak particle velocity versus scaled range curve developed from the FWD testing at the scaled range. We can them estimate the peak particle velocity expected at the critical structure. Knowing the peak particle velocity at the frequency of the roller, we then enter the criteria chart (Figure 4-1) and read a zone at the intersection of the roller frequency and peak particle velocity: RED ZONE, YELLOW ZONE, or GREEN ZONE.

Upon the completion of routine testing and analysis of the deflection data, the SMO sends a memo to the requesting District engineer. The memo includes a recommended design embankment modulus along with any additional information that may be beneficial to the design engineer. In future projects where vibratory sensitive areas are assessed, the memo should also recommend vibratory levels. If the intersection is in the RED ZONE, vibratory compaction should not be allowed. If the intersection is in the YELLOW ZONE, vibratory compaction may be allowed, but the Department should be prepared to field complaints from the public arising from possible annoyance. If the intersection is in the GREEN ZONE, operations should proceed as normal with few, if any, complaints expected from the public.

4.1.4 Buried Sructures

Because Rayleigh waves decay exponentially with depth, most of the associated energy is restricted to near the surface. The practical maximum depth of penetration of the wave is approximately equal to one wavelength.

An appropriate criterion for a fragile buried structure is the RED ZONE, because the concern is that the buried structure might suffer some structural damage that would affect its performance. This criterion is based upon fragile infrastructure such as clay pipe; most modern infrastructure such as culverts, conduits, and communication cables may sustain an even higher level of ground motion without damage. Because the PPV decays exponentially with depth, the RED ZONE distance from the buried structure depends upon the depth of buried structure. By applying Equation 2-2, we can calculate a conservative RED ZONE distance as a function of depth for the characteristics of the roller used. Vibration is not recommended within a range from the buried structure equal to the RED ZONE at the depth of burial of the structure. Figure 4-3 shows an example plot illustrating the application of the criterion to a buried structure.

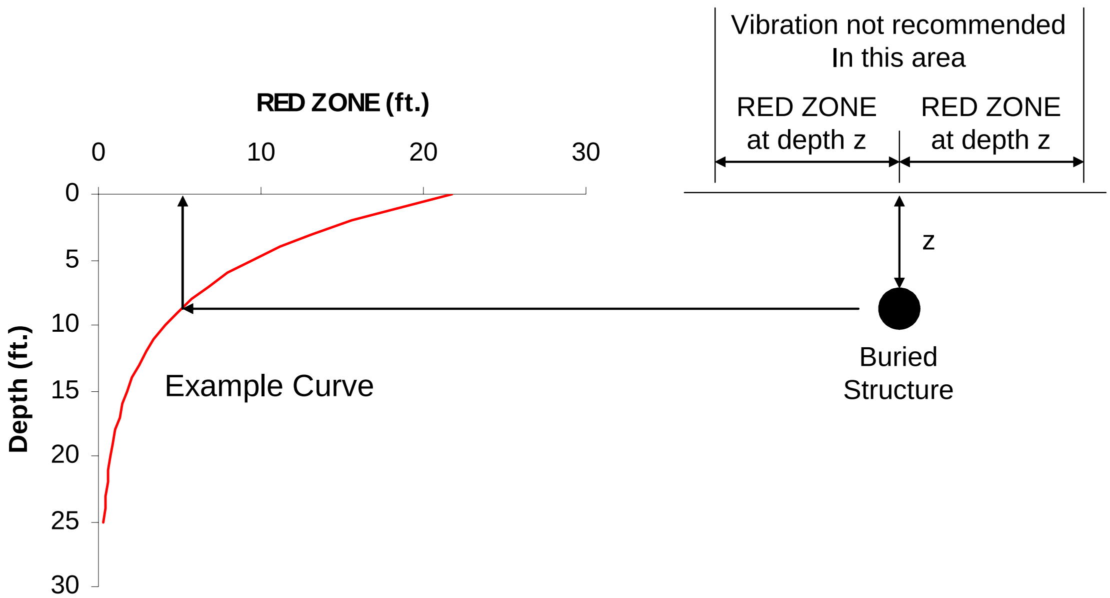

Figure 4-3. Example illustrating application of criteria to buried structure

4.2 Validation Testing

4.2.1 Site Description

Validation testing was conducted on September 5, 2006, at the State Materials Office (SMO) in Gainesville. The purpose of this testing was to validate that preconstruction FWD data could be used to develop an upper-bound ground motion predictor using energy scaling principles.

The SMO reconstructed six lanes of pavement for Heavy Vehicle Simulator (HVS) accelerated pavement testing. A sketch of the HVS test track area is presented in Figure 4-4. The typical pavement sections prior to reconstruction are shown in Figure 4-5. Lanes 2 through 5 were part of a previous flexible pavement HVS experiment, while Lanes 6 and 7 were used in a previous whitetopping experiment. The SMO contracted with Whitehurst Paving to mill and replace approximately 4 inches of HMA on Lanes 2, 3, 4, and 5. On Lanes 6 and 7 Whitehurst removed the existing Portland cement concrete slabs and milled the underlying HMA surface to leave approximately 1½ inch of HMA. The structure of the pavement sections immediately to the east and west of the HVS test tracks are also shown in Figure 4-5.

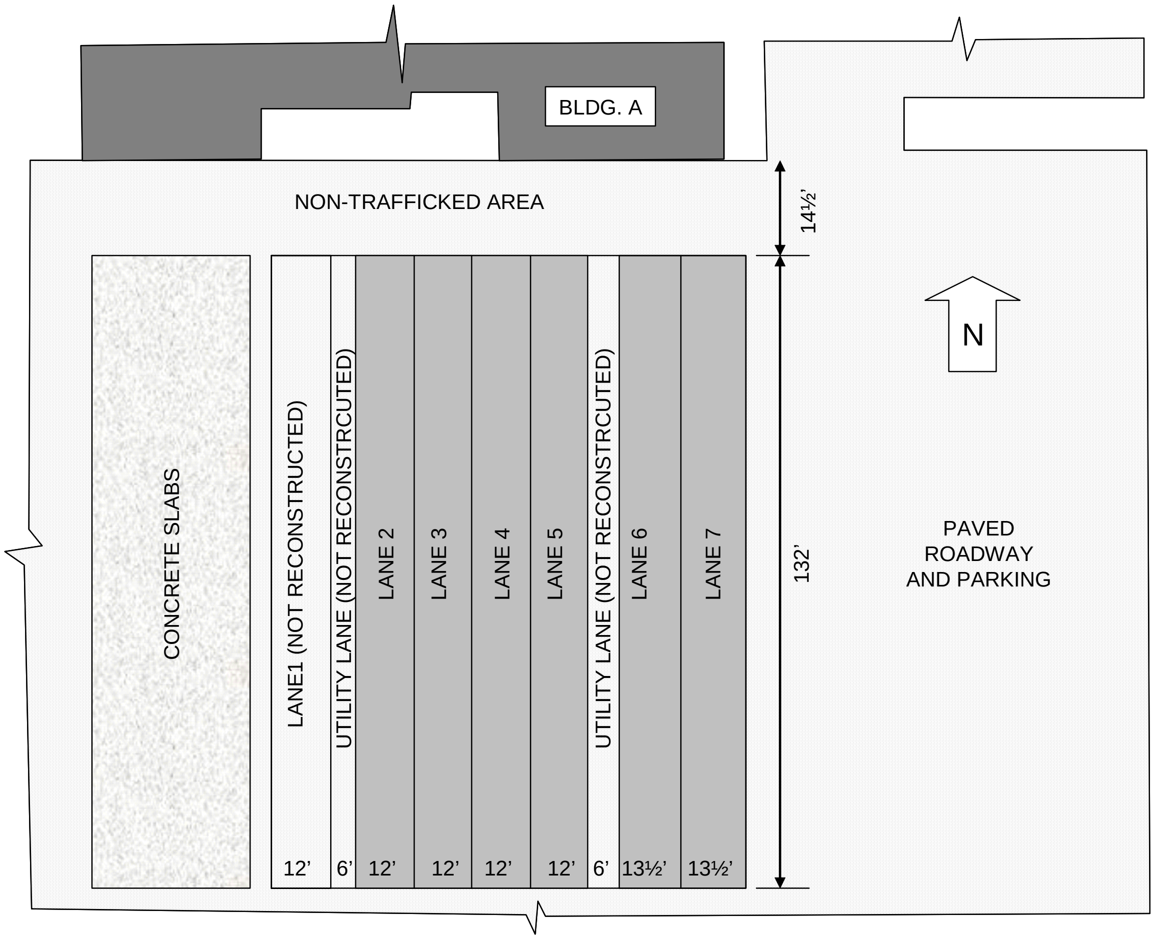

Figure 4-4. General layout of the HVS test track area

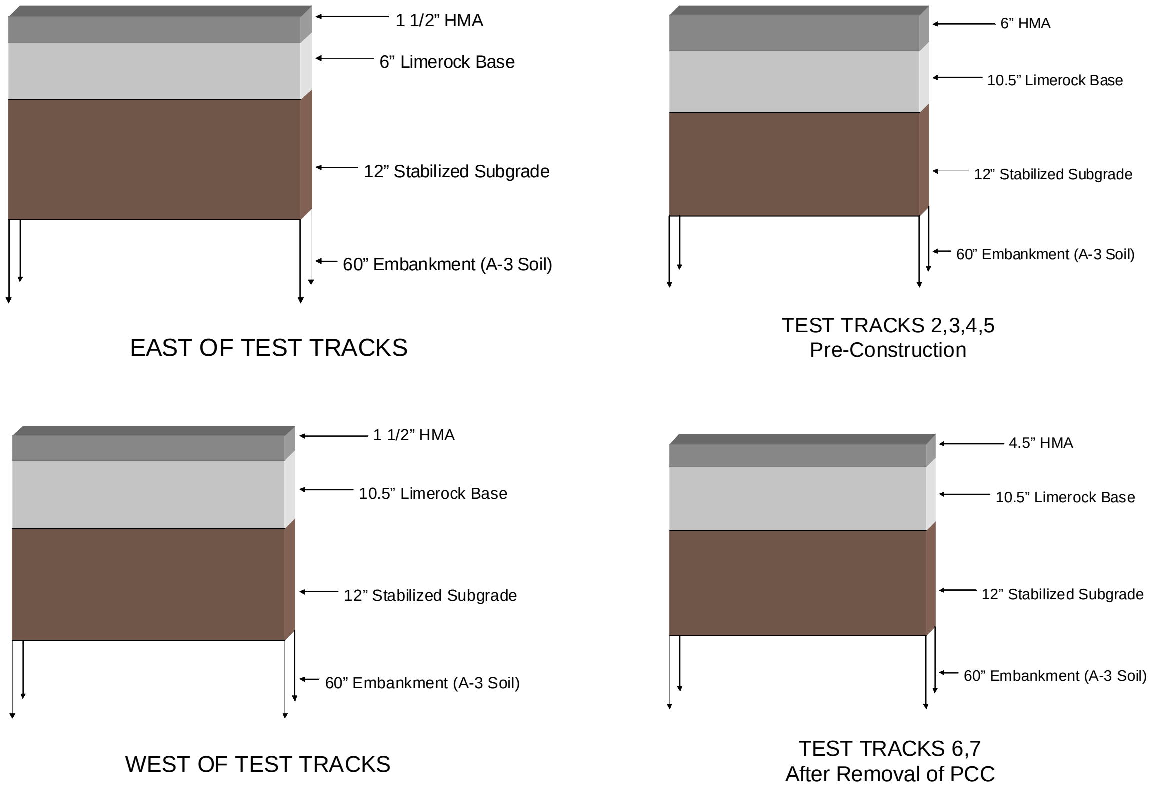

Figure 4-5. Typical pavement sections

Prior to reconstruction of the test sections, a series of FWD tests were conducted at the locations shown in Figure 4-6. FWD testing was not conducted in lanes 1, 6, or 7--lane 1 was not scheduled for reconstruction, and lanes 6 and 7 still had the whitetopping in place at the time the testing was conducted. For each of these tests, the full FWD displacement-time histories were recorded.

4.2.2 Test Description

During the paving operations, six FDOT vibration monitors were used: four in the test track, one at the pavement foundation, and one inside the building as shown in Figure 4-7. The four vibration monitors on the test track remained in place throughout the paving process. This resulted in vibration signatures at varying ranges as the compaction progressed from one side of the HVS track to other. The two monitors near the building (one inside, one outside) were moved by the research team as compaction proceeded from one lane to another.

Safety cones were placed around the monitors in the test track as a safety precaution as shown in the photograph in Figure 4-8. The stationary monitors were rigidly attached to the asphalt surface using bolts drilled into the asphalt. During paving operations, each monitor was covered with a 5-gal plastic bucket to protect it from HMA and overheating in the hot sunshine. The distances from the stationary monitors to the centerlines of the paving lanes are listed in Table 4-2. The building monitors, which were moved as paving progressed from lane to lane, were held in place with sandbags to ensure direct coupling to the ground.

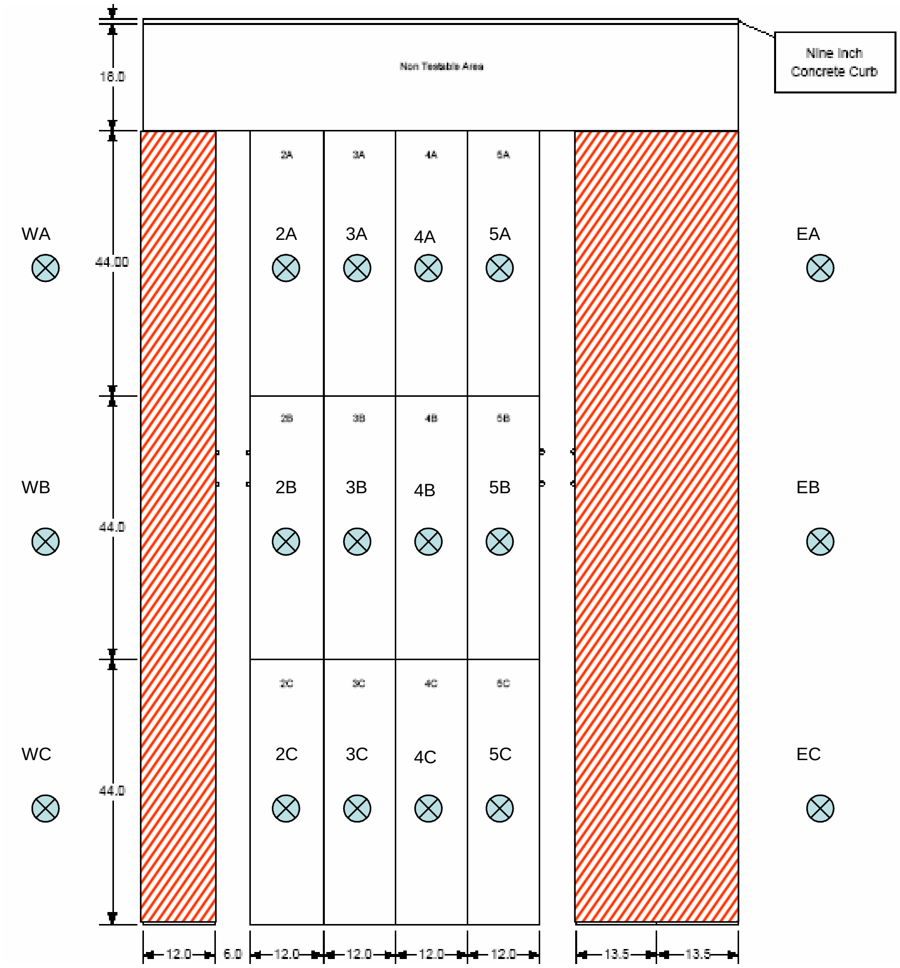

Figure 4-6. Locations of pre-construction FWD testing

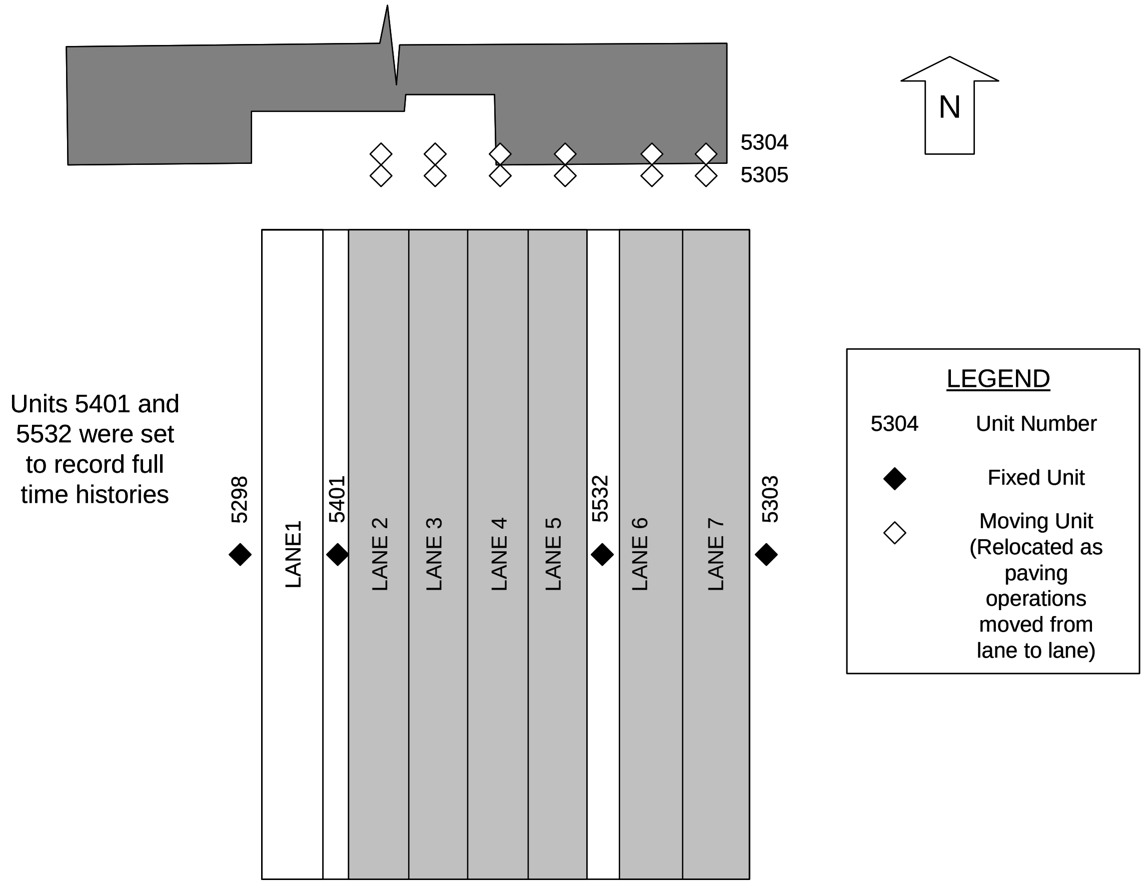

Figure 4-7. Location of vibration monitors

Table 4-2. Distances from vibration monitors to centers of paving lanes

	Distance from Centerline of Lane, ft					
Unit	Lane 7	Lane 6	Lane 5	Lane 4	Lane 3	Lane 2
5298	87 3/4	74 1/4	55 1/2	431/2	31 1/2	19 1/2
5401	77 1/4	63 3/4	45	33	21	9
5532	23 1/4	9 3/4	9 3/4	21 3/4	33 3/4	45 3/4
5503	10 1/4	23 3/4	42 1/2	54 1/2	66 1/2	78 1/2

Whitehurst Construction used a conventional paving operation to surface the lanes (Figure 4-9). A Caterpillar CB-634C vibratory roller, shown in Figure 4-10, was used to compact the mat. The characteristics for this vibratory roller are presented in Table 4-3. The roller was operated at low amplitude and low force. The ground speed of the roller during compaction averaged about 2½ miles per hour.

Figure 4-8. Typical vibration monitor with protective cones (bucket removed)

Figure 4-9. Paving operations

Figure 4-10. Caterpillar CB-643C vibratory roller used for dynamic compaction

Table 4-3. Operating characteristics of Caterpillar CB-634C roller

Characteristic	Value
Operating Weight	28,160 lbs
Maximum Travel Speed	7.6 mph
Drum Width	84 inches
Drum Diameter	52 inches
Frequency	44 Hz
Nominal Amplitude (High)	0.041 inch
Nominal Amplitude (Low)	0.015 inch
Centrifugal Force (Maximum)	35,745 lbs
Centrifugal Force (Minimum)	13,039 lbs

4.2.3 Test Results

The vibration testing results are summarized in Table 4-4. The dominant frequency of the vibration was approximately 40 Hz. In Figure 4-11, the PPVs have been plotted versus the un-scaled range to the center of the paving lane. These data are consistent with the expected results and validate that the vibration monitors appear to have been functioning properly during the paving operations.

Table 4-4. Vibration results summary

Instrument	Lane	Distance to Center of Lane, ft	Trigger Time	Travel Direction	PPV, in/s			Dominant Frequency, Hz		
					Trans	Vert	Long	Trans	Vert	Long
5401	2	9	13:53:19	North	0.341	0.634	0.472	40.3	40.3	40.3
5401	2	9	13:51:59	South	0.111	0.267	0.165	40.0	40.1	40.1
5401	2	9	13:51:23	North	0.351	0.736	0.520	40.4	40.4	40.4
5401	2	9	13:50:48	South	0.269	0.583	0.421	40.0	40.1	40.1
5401	2	9	13:50:14	North	0.231	0.531	0.417	40.5	40.5	40.5
5401	3	21	13:18:36	North	0.119	0.216	0.172	40.4	40.4	40.4
5401	3	21	13:17:58	South	0.166	0.236	0.224	40.0	40.1	40.1
5401	3	21	13:16:56	South	0.114	0.318	0.265	40.0	40.3	40.3
5401	3	21	13:16:22	North	0.099	0.194	0.139	40.5	40.4	40.4
5401	4	33	12:47:03	North	0.097	0.169	0.195	40.0	40.0	40.0
5401	4	33	12:46:33	South	0.119	0.104	0.132	40.1	40.1	40.1
5401	4	33	12:45:36	South	0.080	0.109	0.161	40.3	40.0	40.3
5401	4	33	12:45:07	North	0.049	0.096	0.083	40.0	80.1	40.0
5401	5	45	12:23:17	South	0.032	0.166	0.056	80.1	40.1	40.1
5401	5	45	12:22:08	South	0.043	0.177	0.053	40.1	40.1	40.1
5401	5	45	12:21:35	North	0.037	0.137	0.048	40.0	40.3	80.3
5401	6	63.75	11:15:30	North	0.017	0.024	0.038	40.4	40.1	40.1
5401	6	63.75	11:14:21	North	0.043	0.120	0.068	40.3	40.1	40.1
5401	6	63.75	11:13:38	South	0.024	0.054	0.039	40.1	40.1	40.1
5401	7	77.25	10:56:19	South	0.026	0.076	0.026	40.0	40.1	40.1
5401	7	77.25	10:55:50	North	0.019	0.027	0.021	40.1	40.1	40.1
5401	7	77.25	10:54:29	North	0.022	0.058	0.025	40.0	39.9	39.9
5401	7	77.25	10:53:55	South	0.026	0.084	0.019	40.3	40.3	40.3
5401	7	77.25	10:53:23	North	0.021	0.054	0.021	40.1	40.0	40.0
5401	7	77.25	10:52:56	South	0.013	0.039	0.021	40.4	40.4	40.4
5401	7	77.25	10:52:25	North	0.026	0.057	0.036	40.1	40.1	40.1
5401	7	77.25	10:51:52	South	0.026	0.029	0.018	40.3	40.5	40.3
5401	7	77.25	10:51:14	North	0.015	0.029	0.029	40.0	40.3	40.1
5401	7	77.25	10:50:24	South	0.022	0.032	0.018	39.9	39.9	40.0
5532	5	9.75	12:23:16	South	0.216	0.854	0.445	39.9	40.0	40.0
5532	5	9.75	12:22:09	South	0.187	0.780	0.449	39.9	40.0	40.0
5532	5	9.75	12:21:36	North	0.201	0.650	0.274	40.4	40.4	40.4
5532	6	9.75	11:15:31	North	0.238	0.811	0.364	40.4	40.4	40.3
5532	6	9.75	11:14:22	North	0.200	0.713	0.344	40.0	40.1	40.1
5532	6	9.75	11:13:47	South	0.234	0.724	0.329	40.5	40.4	40.1
5532	4	21.75	12:47:05	North	0.119	0.421	0.409	40.0	39.9	40.0
5532	4	21.75	12:46:33	South	0.147	0.385	0.333	40.1	40.1	40.1
5532	4	21.75	12:45:36	South	0.104	0.361	0.365	40.3	40.3	40.3
5532	4	21.75	12:45:07	North	0.076	0.166	0.104	40.1	40.0	40.0
5532	7	23.25	10:56:20	South	0.081	0.461	0.199	40.1	39.9	40.0
5532	7	23.25	10:55:50	North	0.040	0.180	0.090	40.0	39.9	40.0
5532	7	23.25	10:54:29	North	0.077	0.377	0.180	39.8	39.8	39.9
5532	7	23.25	10:53:55	South	0.081	0.480	0.217	40.3	40.3	40.3
5532	7	23.25	10:53:23	North	0.083	0.409	0.183	39.9	39.9	40.0
5532	7	23.25	10:52:55	South	0.087	0.318	0.137	40.1	40.1	40.1
5532	7	23.25	10:52:24	North	0.084	0.199	0.069	40.0	40.0	40.0
5532	7	23.25	10:51:52	South	0.037	0.131	0.056	40.1	40.1	40.1
5532	7	23.25	10:51:14	North	0.049	0.180	0.096	40.3	40.1	40.1
5532	7	23.25	10:50:29	South	0.073	0.292	0.065	40.0	40.0	40.1
5532	3	33.75	13:18:39	North	0.041	0.220	0.056	40.5	40.3	40.4
5532	3	33.75	13:17:59	South	0.063	0.202	0.056	40.1	40.3	40.1
5532	3	33.75	13:16:55	South	0.061	0.222	0.075	40.3	40.3	40.1
5532	3	33.75	13:16:23	North	0.040	0.123	0.048	40.1	40.1	40.4
5532	2	45.75	13:53:21	North	0.033	0.149	0.071	40.1	40.1	40.1
5532	2	45.75	13:51:58	South	0.033	0.173	0.074	40.3	40.3	40.1
5532	2	45.75	13:51:24	North	0.031	0.144	0.078	40.3	40.3	40.3
5532	2	45.75	13:50:49	South	0.059	0.163	0.102	40.4	40.5	40.4
5532	2	45.75	13:50:16	North	0.026	0.134	0.052	40.3	40.3	40.3

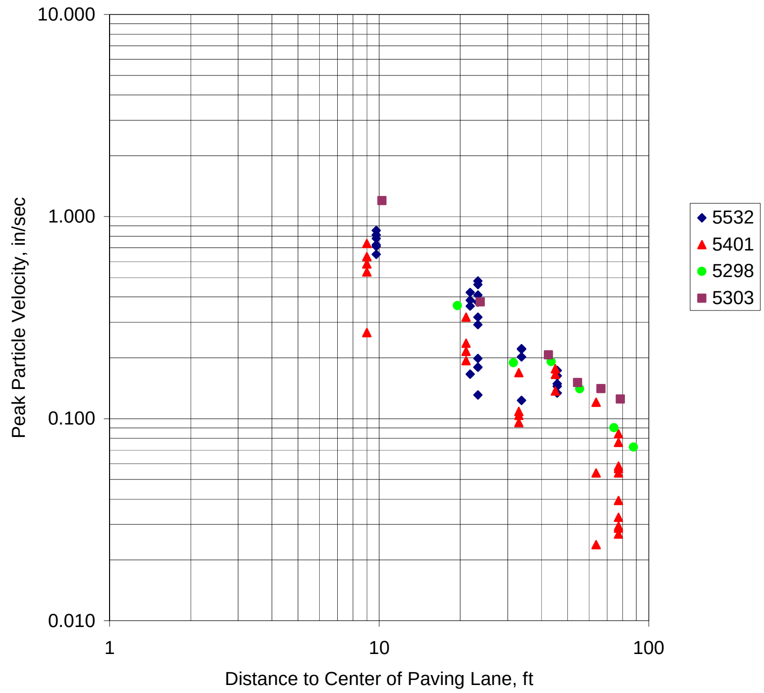

Figure 4-11. Peak velocity versus un-scaled range for the stationary monitors

4.2.4 Data Analysis

The data were analyzed using the principles of square root scaling. Figure 4-12 shows the same data contained in Figure 4-11, only the ranges have been scaled by the reciprocal of the square root of the peak FWD energy. Two potential curves were fit through the data using the method of least squares: one was a linear relationship, the other a second order polynomial function. The results of the curve fits are presented in Figure 4-13. The correlation coefficient values were 0.968 for the straight line and 0.970 for the polynomial, so it appears that either is valid. In all subsequent analyses, the polynomial fit was used because it was a slightly better representation of the data. This curve represents the upper-bound predictor of ground motions for the site.

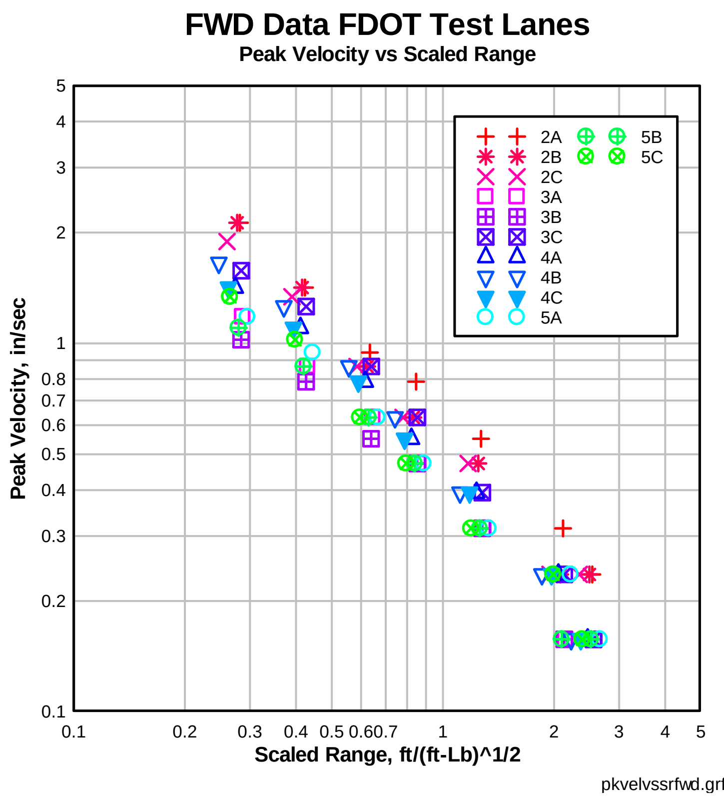

Figure 4-12. PPV versus scaled range

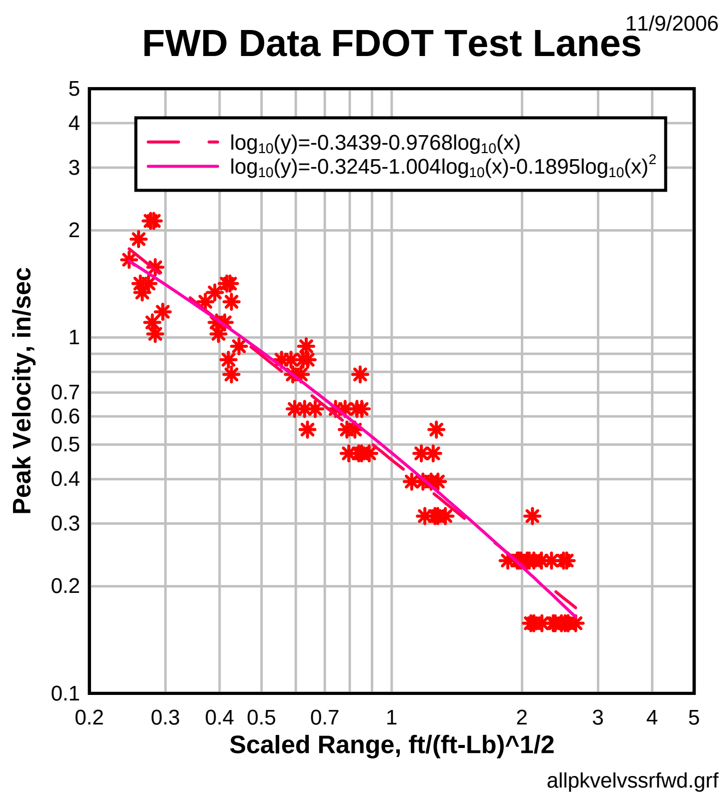

Figure 4-13. Curve fit through FWD ground motion data

At minimum load and displacement, the energy from the vibratory roller is 13,039× 0.015/12 = 16.3 ft-lb. The estimate of the speed of the compactor at the test site was 2.5 mph which translates to 1 inch per period or 51 impacts for the transit of one diameter. With the resulting total energy from these two levels the site data were scaled and compared to the predictor. The result is shown in Figure 4-14. Note that the predictor upper bounds the data, which is the correct characteristic for the predictor.

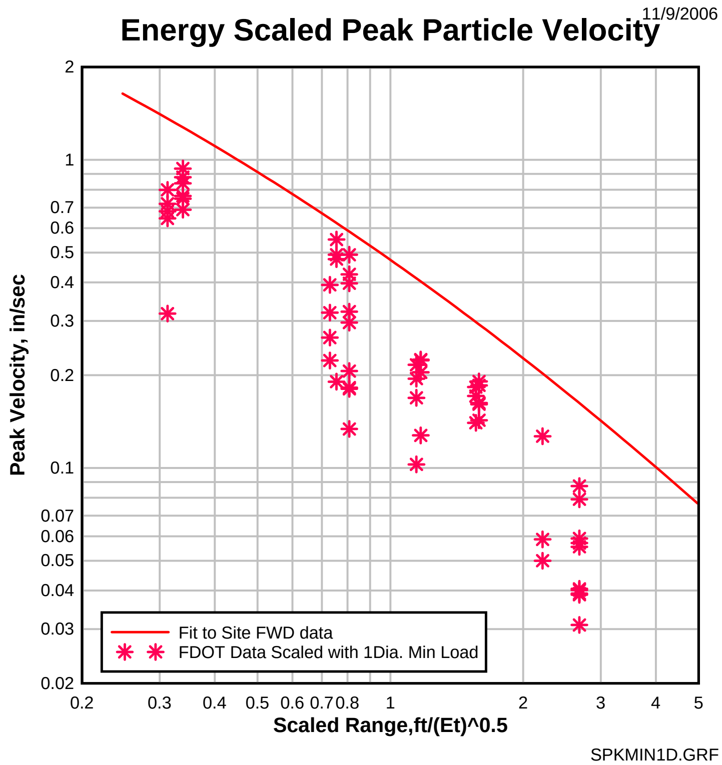

Figure 4-14. Predictor curve from FWD test versus measured ground motions from roller

5 IMPLEMENTATION

5.1 Software Implementation

The procedures described in Chapter 4 were implemented in a Microsoft Excel® workbook "Vibration Calculator.xls". The spreadsheet prompts the user for the required input information, reads a user-selected FWD displacement time history file, performs the required numerical calculations, and estimates the RED, YELLOW, and GREEN ZONES for the project. The workbook is described in more detail in the following sections.

5.1.1 Workbook Organization

The Vibration Calculator workbook contains a number of worksheets identified by the colored tabs at the bottom of the workspace. Each of these worksheets is described below

5.1.1.1 User's Guide Worksheet

The User's Guide worksheet provides a basic description of the workbook and the several worksheets that make up the workbook. The User's Guide also provides basic instructions for importing FWD data into the workbook.

5.1.1.2 Basic Inputs Worksheet

The Basic Inputs worksheet (Figure 5-1) provides a simple report of the results produced by the workbook. Information about the project such as the project Financial Information Number (FIN), county section number, location, and direction can be stored and edited here.

This worksheet also has a note about the currently selected roller specifications. If custom values were entered, "Using Custom Roller Values" will appear below the comments. Otherwise, "Using Default Roller Values" will appear instead.

The results of the calculations appear to the right of the editable fields. Here, ranges in feet for each response level are shown.

Three buttons appear to the left and below the editable fields. The first is used to load Dynatest FWD time-history data, while the second is used to load JILS time-history data. The third button clears all input data from the spreadsheet.

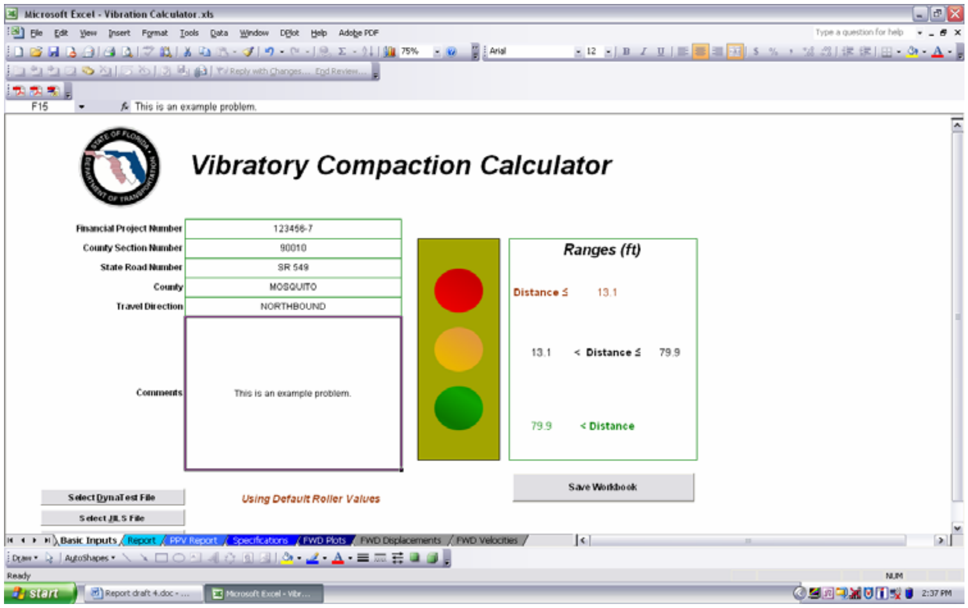

Figure 5-1. Screen shot of Basic Inputs worksheet

Dynatest software writes the time history files as a Microsoft Access™ database file. For Dynatest files, the Access file must be extracted to a Microsoft Excel® worksheet. To do this, open the file in Access™. Right-click the "Histories" table, then select "Export…" from the pop-up menu. Enter a name for the file, and select "Microsoft Excel 97-2003 (*.xls)" from the "Save as type:" pull-down menu. Navigate to the directory the file should be saved under, and click "Export."

The JILS software writes the time history data in a text file format that can be readily imported to Microsoft Excel®. For JILS files, ensure that the Excel® worksheet is saved with the worksheet containing the time-history data selected. This worksheet should have the project number as its name.

Once preparations are complete, select the Basic Inputs worksheet and click the appropriate button. A menu will ask for the file to load. Navigate to the correct directory, select the file, and click "OK". A popup window will appear displaying the program's progress through the file. Once the progress reads "100%", the popup window will disappear, and the Basic Inputs worksheet will be displayed. At this point, all calculations are complete. Changing roller specifications will show the changes on the Basic Inputs worksheet.

The user may elect to save the entire spreadsheet by selecting the “Save Workbook” button at the lower right corner of the screen. The default file name given by the program contains the county name, county section number and the text “vib”. The default name and folder can be changed using the resulting Windows® “Save File” dialog box.

5.1.1.3 PPV Report Worksheet

The PPV (Peak Particle Velocity) Report worksheet (Figure 5-2) presents a plot of the limiting criteria for each response level in terms of peak particle velocity versus roller frequency. To the right of that lies the bounding predictor curve created from the FWD data. This curve is compared to the roller's estimated peak particle velocity values to estimate a scaled range. The black curve is the best fit curve through the data, and the red curve is the upper bound 95 percent confidence interval used in calculating the critical distances.

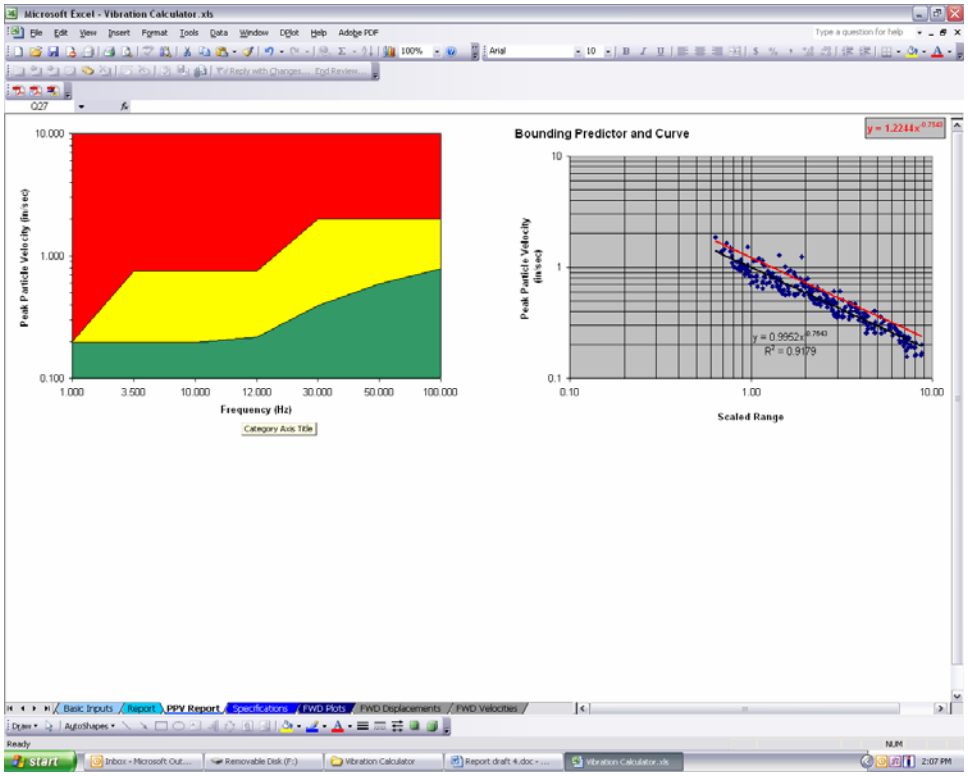

Figure 5-2. Screenshot of PPV Report worksheet

5.1.1.4 Specifications Worksheet

The Specifications worksheet (Figure 5-3) stores all relevant roller and FWD information and can be edited. The roller's drum diameter, load, amplitude, and frequency can be set under "Roller Specifications." A check box below these fields will indicate whether default values are being used. To change these fields, the box must be unchecked. Changes made here will be immediately reflected in the Basic Inputs and Report worksheets.

The only aspect of the FWD that can be changed is the load used for the test. This can be altered below the roller specifications. Note that changes here will not take effect until another FWD file is loaded from the Basic Inputs worksheet.

5.1.1.5 FWD Plots Worksheet

The FWD Plots worksheet, shown in Figure 5-4, presents time history plots of displacement, velocity, and peak energy for each production drop.

5.1.1.6 Report

The Report worksheet (Figure 5-5) is designed to be a printer-friendly, one page report of all relevant data in the project. Select this worksheet and select "Print…" from the file menu, then click "OK" to print a report to the currently selected printer.

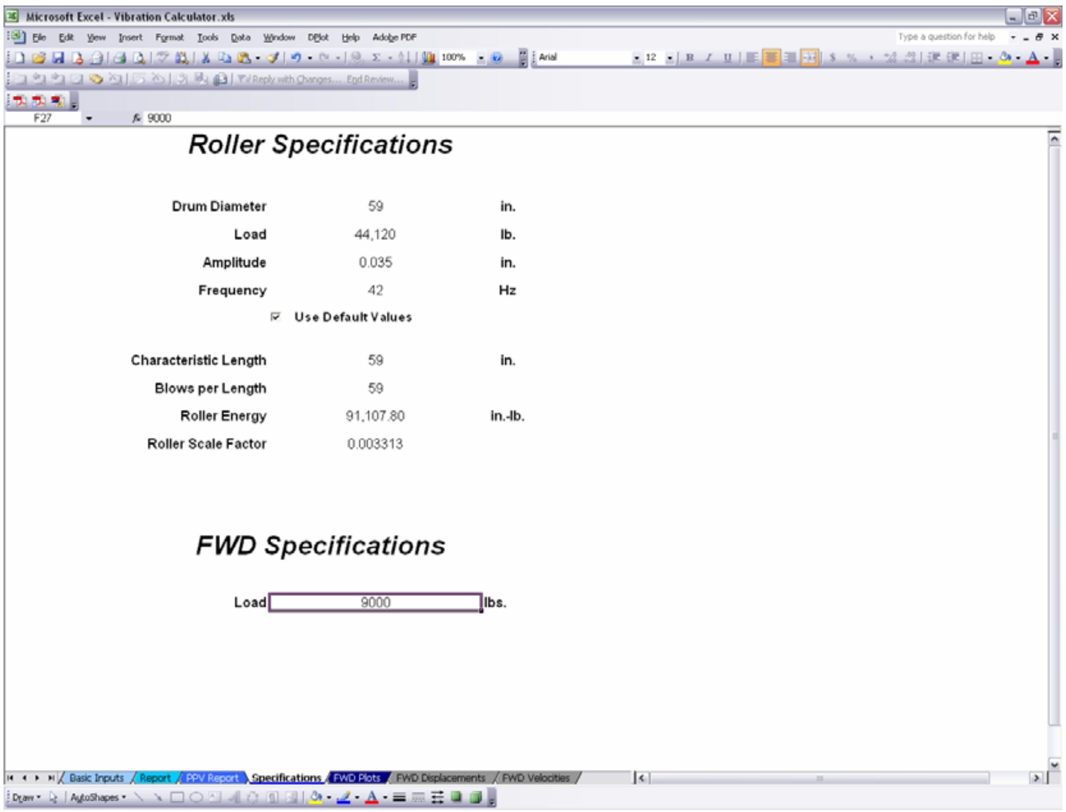

Figure 5-3. Screenshot of Specifications worksheet

\

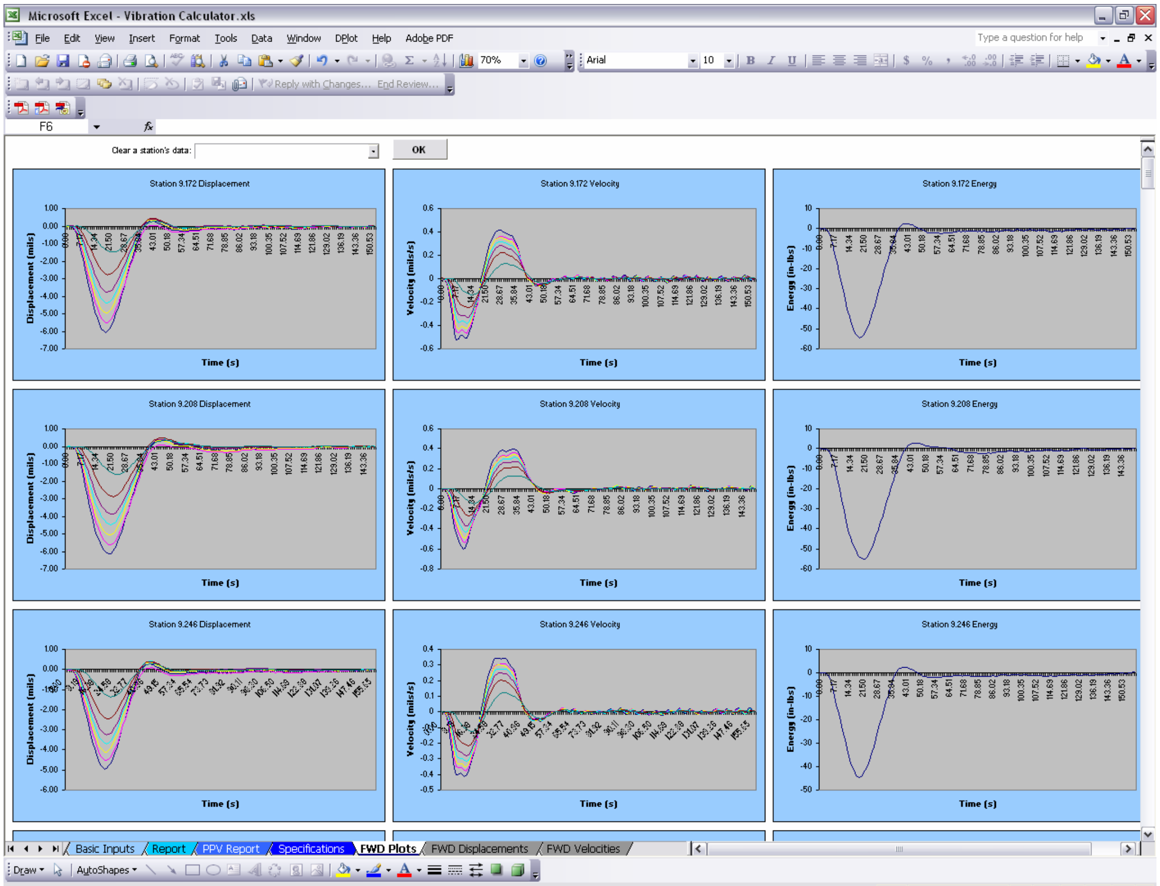

Figure 5-4. Screenshot of FWD Plots worksheet

Non-Destructive Testing Vibratory Compaction Criteria Report

PROJECT INFORMATION **DATE** 02/16/07

FIN:	123456-7
COUNTY:	MOSQUITO
SECTION ID:	90010
STATE ROAD NUMBER:	SR 549
DIRECTION:	NORTHBOUND
COMMENTS:	This is an example problem.

ROLLER INFORMATION **FWD INFORMATION**

☑ ***Default roller was used.*** **LOAD (lbf):** 9000

Default roller was not used.

LOAD (lbf):	44,120
AMPLITUDE (in):	0.035
FREQUENCY (Hz):	42
DRUM DIAMETER (in):	59

VIBRATION CRITERIA: SURFACE STRUCTURES

RED ZONE (ft):	Distance (ft) ≤ 13.1
YELLOW ZONE (ft):	13.1 < Distance (ft) ≤ 79.9
GREEN ZONE (ft):	Distance (ft) > 79.9

Conditions in the RED ZONE should be avoided to prevent possible architectural or structural damage to buildings. Conditions in the YELLOW ZONE are acceptable; however, the department should be prepared to receive complaints from persons who may be annoyed by the vibration. Operations in the GREEN ZONE should incur few, if any, complaints from the public.

VIBRATION CRITERIA: BURIED STRUCTURES

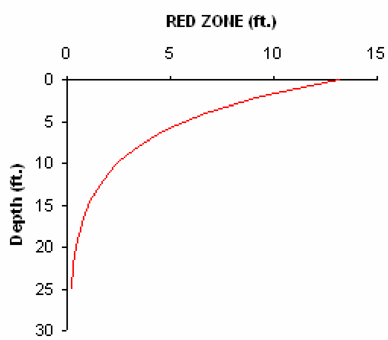

For fragile buried structures, the plot to the left shows the RED ZONE as a function of depth. Enter the plot at the depth of the buried structure and estimate the RED ZONE from the curve. Vibratory compaction is not recommended within a distance equal to the RED ZONE from the buried structure.

Figure 5-5. Report worksheet

5.2 Example Problem

5.2.1 Project Description

The project selected for an example problem was SR 15 from Milepost 9.100 to Milepost 11.700 in Orange County. The County Section Number was 75080, and the Financial Identification Number was 239266-3. The roadway generally consists of two 13-ft wide travel lanes and is functionally classified as an Urban Minor Arterial. The pavement structure was unknown.

5.2.2 Pre-Design Evaluation

The roadway was tested by the State Materials Office on November 13, 2006, using a JILS FWD. The SMO's standard procedures for pre-design evaluation were followed with the exception that the displacement-time histories were recorded for each drop. A total of 72 production drops were performed on the roadway, and the resulting deflection data are plotted in Figure 5-6. The design embankment resilient modulus was determined to be 20,000 psi from the test results. These results are documented in a memorandum from James H. Greene, P.E., of Applied Research Associates, Inc., to Timothy Keefe, District 5 Project Manager.

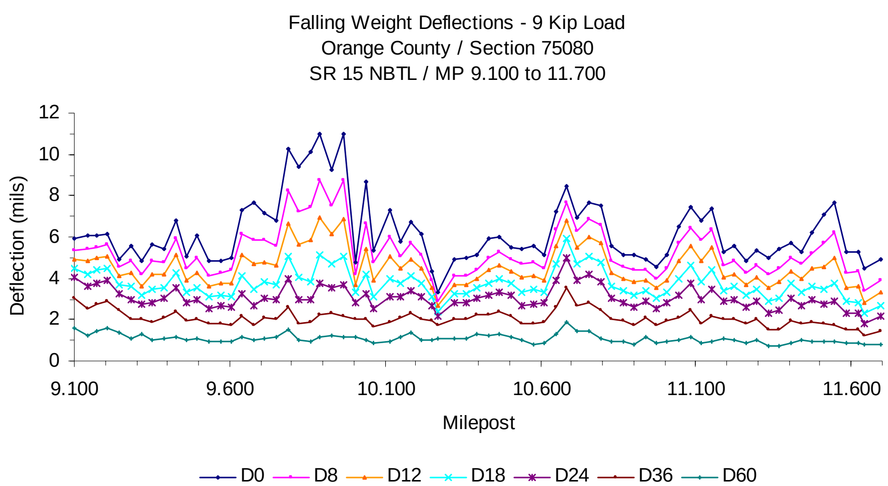

Figure 5-6. Peak deflection data from SR 15

5.2.3 Vibration Characterization

The displacement-time histories were analyzed using the Vibration Calculator workbook. The resulting bounding PPV versus scaled range curve is shown in Figure 5-7. This chart will be used to predict the expected vibration magnitudes (PPV) during HMA compaction.

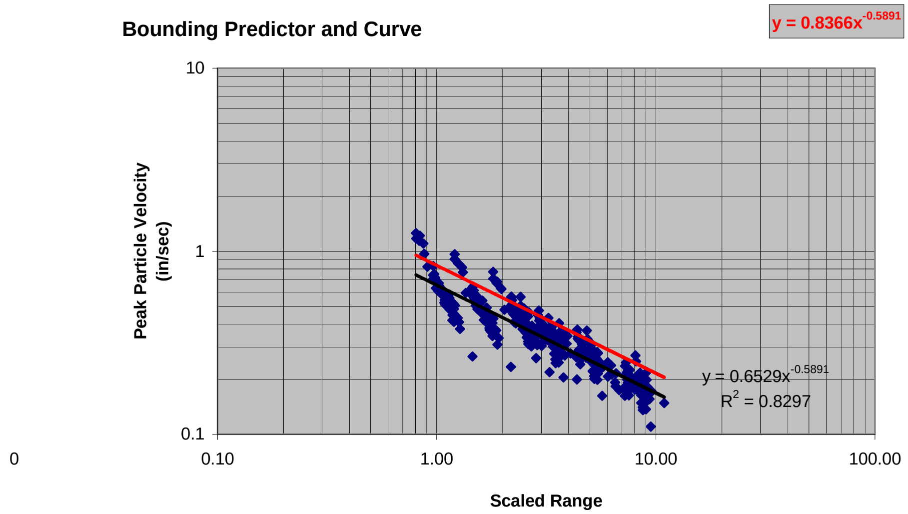

Figure 5-7. FWD bounding predictor curve for SR 15

5.2.4 Roller Characteristics

The default roller values for the Ingersoll-Rand DD-158HFA as given in Table 4-1 were used for these calculations. Table 5-1 lists the input parameters and calculated energy and scale factors for this roller.

Table 5-1. Roller characteristics, SR 15

Parameter	Value
Peak Load (lbf)	44,120
Amplitude, (inches)	0.035
Frequency, (Hz)	42
Peak Energy, (in-lbs)	91,108
Scale Factor	0.003313

5.2.5 Vibration Criteria

As tabulated in Table 5-1, the roller frequency for the example problem is 42 Hz. Entering Figure 4-1 at 42 Hz on the horizontal axis, we read that the GREEN-YELLOW threshold is at a PPV of approximately 0.51 in/sec and the YELLOW-RED threshold is at 2 in/sec. Using the upper bound confidence interval in Figure 5-7, the following critical ranges were calculated:

Critical Threshold	PPV, in/sec	Scaled Range	Range, ft
GREEN/YELLOW	0.51	1.700	57.9
YELLOW/RED	2.00	0.3366	5.7

Therefore the RED ZONE is within 6 feet from the center of the paving lane, the YELLOW ZONE includes ranges between 6 and 58 ft, and the GREEN ZONE includes any distance greater than 58 feet. The report page for the example problem is shown in Figure 5-8. The plot at the lower right of the report page shows the RED ZONE as a function of depth, which can be used to determine recommended safe vibratory compaction distances from a fragile buried structure at a given depth of burial.

5.2.6 Other Examples

A couple of other time-histories files were made available by the SMO for comparison. The first was SR 200 in Nassau County, and the other was pre-construction testing on the Accelerated Pavement Testing tracks at the State Materials Office in Gainesville. Figure 5-9 shows the results of exercising the workbook on these files using the default roller parameters.

Non-Destructive Testing
Vibratory Compaction Criteria
Report

PROJECT INFORMATION **DATE** 02/16/07

FIN:	239266-3
COUNTY:	ORANGE
SECTION ID:	75080
STATE ROAD NUMBER:	SR 15
DIRECTION:	NORTHBOUND
COMMENTS:	This is an example problem.

ROLLER INFORMATION **FWD INFORMATION**

☑ *Default roller was used.* **LOAD (lbf):** 9000

Default roller was not used.

LOAD (lbf):	44,120
AMPLITUDE (in):	0.035
FREQUENCY (Hz):	42
DRUM DIAMETER (in):	59

VIBRATION CRITERIA: SURFACE STRUCTURES

RED ZONE (ft):	Distance (ft) ≤ 5.7
YELLOW ZONE (ft):	5.7 < Distance (ft) ≤ 57.9
GREEN ZONE (ft):	Distance (ft) > 57.9

Conditions in the RED ZONE should be avoided to prevent possible architectural or structural damage to buildings. Conditions in the YELLOW ZONE are acceptable; however, the department should be prepared to receive complaints from persons who may be annoyed by the vibration. Operations in the GREEN ZONE should incur few, if any, complaints from the public.

VIBRATION CRITERIA: BURIED STRUCTURES

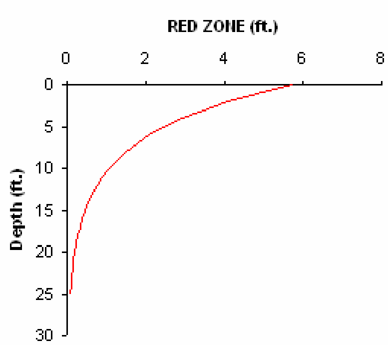

For fragile buried structures, the plot to the left shows the RED ZONE as a function of depth. Enter the plot at the depth of the buried structure and estimate the RED ZONE from the curve. Vibratory compaction is not recommended within a distance equal to the RED ZONE from the buried structure.

Figure 5-8. Report page for example problem

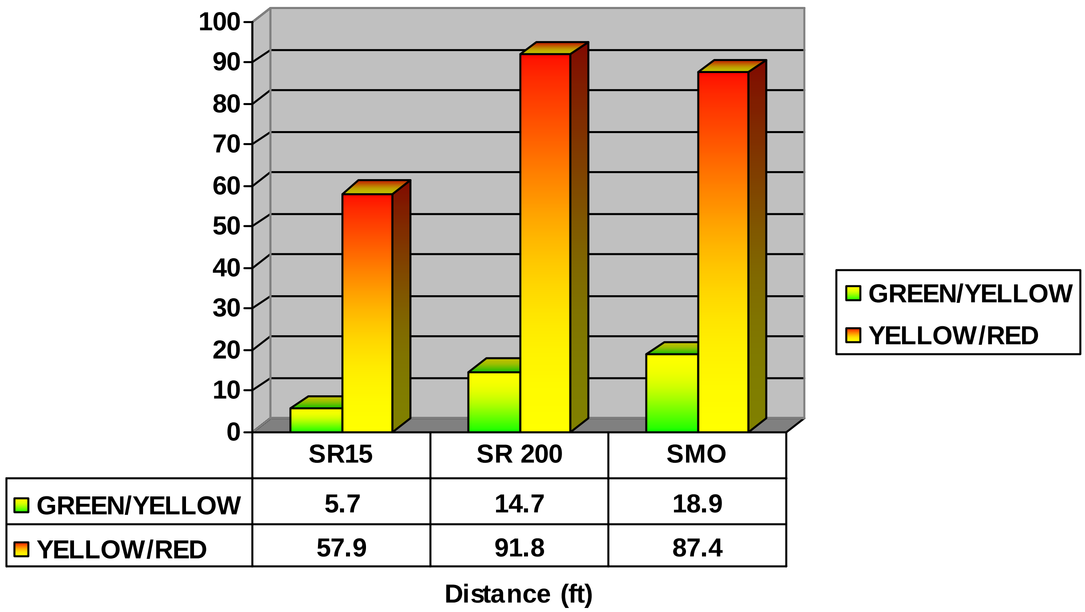

Figure 5-9. Results from example problems

6 CONCLUSIONS AND RECOMMENDATIONS

6.1 Conclusions

It is generally accepted that vibratory rollers for compacting HMA should operate at a frequency and ground speed to impact the mat 10 to 14 times per foot. Vibration amplitude, or vertical distance the drum travels, is also critical. The most effective combination of frequency and amplitude is different for different mixes and lift thicknesses.

Earthborne vibrations from vibratory compaction equipment can be described as single-frequency continuous vibration. A vibratory roller generates approximately 80% of the ground motion in Raleigh and shear waves. Rayleigh wave motion penetrates the ground surface a distance of only one to two wavelengths. The energy per unit volume that generates surface waves decreases proportional the volume of a cylinder. Because the volume of a cylinder is proportional to square of its radius, r^2, the decay is proportional to $1/r^2$.

Human perception of ground vibrations is subjective and depends upon a number of factors. Most routine vibration complaints come from persons who are ill, elderly, or are engaged in a vibration sensitive hobby or activity. Even low level vibrations may cause annoying secondary effects such as rattling of windows, doors, or dishes. While these secondary vibrations may be irritating, they are not likely to cause property damage.

Damage to buildings caused by earthborne vibrations can be categorized as either architectural damage or structural damage. Architectural damage is superficial damage such as hairline cracks in plaster walls or ceilings. Most buildings usually have residual strains as a result of foundation movement, moisture and temperature cycles, poor maintenance, or past construction activities. In some cases, even relatively small levels of vibrations can result in superficial damage. While catastrophic damage to buildings from construction operations are extremely rare, some structural damage such as separation of masonry blocks and cracking in foundations, swimming pools, chimneys, and other sensitive structures may occur in cases where earthborne vibrations exceed threshold levels.

Various Federal, State, and foreign agencies have proposed vibration limit criteria, some intended to mitigate damage to structures, while others are based upon limiting human annoyance. We have selected two of these criteria to form the basis of our recommendations. The criteria are represented as three zones on a plot of peak particle velocity versus vibratory roller frequency:

- The RED ZONE designates a region of the plot were damage to structures is possible.

- The YELLOW ZONE designates a region of the plot where human annoyance is possible, but damage to buildings is unlikely.
- The GREEN ZONE designates the region of the plot were ground motions may or may not be noticeable by persons, but human annoyance is unlikely.

Scaling or normalizing of ground motion is based upon the geometric dispersion of the motion induced by a dynamic source. The energy per unit volume that generates surface waves decreases in proportion to the volume of a cylinder; thus, a square root scaling law is applicable. To normalize the ground motions from the FWD and the vibratory compactor, we have chosen to use the scaling law $R/U^{1/2}$ where R is the range of a point in question and U is the energy input into the system. Procedures were developed to calculate the input energy from the FWD and a vibratory roller; therefore scaled ranges can be used to compare the responses from the two energy sources.

A potentially vibration-sensitive project can be characterized using displacement-time histories from the FWD obtained during routine pre-construction testing. Detailed knowledge of the layering of the pavement structure or the geology of the surrounding site is not required. The requesting District Engineer should identify flexible rehabilitation projects within urban areas or near vibration sensitive structures before the SMO is requested to perform deflection testing. When the requesting Engineer identifies the project as potentially vibration-sensitive, the SMO should record the full FWD displacement time histories on each FWD during pre-design testing. The data are processed to develop a plot of peak velocity versus scaled range for the project. This plot is as an upper bound predictor of ground motion at the site. By knowing (or assuming) a frequency for the vibratory roller, the peak particle velocity can be used to determine whether a given range is within the RED, YELLOW, or GREEN ZONE.

Most of the energy from the wave is restricted to near the surface. Rayleigh waves decay exponentially with depth, and the practical maximum depth of penetration of the Rayleigh wave is approximately equal to one wavelength. These facts were used to develop an estimate of the RED ZONE as a function of depth based upon the known (or assumed) characteristics of the roller. This predictor can be used to restrict vibratory compaction near fragile buried infrastructure.

6.2 Recommendations

Conditions in the RED ZONE should be avoided to prevent possible architectural or structural damage to buildings. Conditions in the YELLOW ZONE are acceptable; however, the department should be prepared to receive complaints from persons who may be annoyed by the vibration. Vibration in the GREEN ZONE should incur few, if any, complaints from the public. For fragile buried structures, vibration should be avoided within a distance equal to the RED ZONE at the depth of burial.

The distances associated with the RED, YELLOW, and GREEN ZONES could be plotted on aerial photographs of the projects to determine which structures may be adversely affected by vibratory compaction.

The methods and procedures described in this report have not been fully validated, and further calibration of the method may be required. We recommend that the results from this research be monitored, and if necessary, the calibration of the methods be performed to better reflect field conditions.

7 REFERENCES

American Association of State Highway and Transportation Officials. 1993. *AASHTO Guide for the Design of Pavement Structures*. Publication GDPS-4, American Association of Highway and Transportation Officials, Washington, DC.

Amick, H. 1999. "A Frequency Dependent Soil Propagation Model." Presented at International Society for Optical Engineering Conference on Current Developments in Vibration Control for Optomechanical Systems, Denver, CO July 1999, www.cganda.com/pdf/Amick-SPIE99.pdf, accessed August 12, 2005.

Amick, H. and M. Gendreau. 2000. "Construction Vibrations and Their Impact on Vibration-Sensitive Facilities." *Proceedings of the Sixth Construction Congress*, American Society of Civil Engineers, Orlando, Florida, February, 2000, pp. 758-767.

Briaud, J.L. and J. Seo. 2003. *Intelligent Compaction: Overview and Research Needs,* Texas A&M University, Bryan, TX, accessed at webs1.uidaho.edu/bayomy/trb.afh60/IntCompaction_Briaud_September2004_pdf on August 16, 2005.

Caterpillar. 2005. "Intelligent Compaction." Ucs.iastate.edu/mnet/_repository/2005/asphalt/pdf/programfiles/Intelligent%20Compaction.pdf, accessed August 16, 2005.

Dowding, C. H. 1996. *Construction Vibrations,* Prentice Hall, Upper Saddle River, NJ.

CTC and Associates LLC. 2003. Construction Vibrations and Historic Buildings Transportation Synthesis Report, Wisconsin Department of Transportation, www.dot.wisconsin.gov/library/research/docs/tsrs/tsrconstructionvibration.pdf. Accessed May 17, 2005.

Florida Department of Transportation. 2004. Standard Specifications for Road and Bridge Construction, Tallahassee, FL.

Hendriks, R. *Transportation Related Earthborne Vibrations (Caltrans Experiences).* TAV-02-01-R9601, California Department of Transportation, Sacramento, California, 2002.

Henwood, J. T. and K. Y. Haramy. 2002. Vibrations Induced by Construction Traffic: A Historic Case Study. Presented at Geophysics 2002, April 15-19, 2002, www.dot.ca.gov/hq/esc/geotech/gg/geophysics2002/043henwood_construction_vibrations.pdf, accessed May 17, 2005.

Holtschucher, C. and H. Lee. 2007. *2006 Resilient Modulus of Roadbed Soils Facts and Figures*, Research Report FL/DOT/SMO/07-502, State Materials Office, Florida Department of Transportation, Gainesville, FL.

Hunaidi, O. 2000. Traffic Vibrations in Buildings, Construction Technology Update No. 39, National Research Council of Canada, Ottawa.

Moore, Walt. (2006). "Intelligent Compaction: Outsmarting Soils and Asphalt," www.constructionequipment.com, accessed September 19, 2006.

Nichols, H.R., C.F. Johnson, and W. I. Duvall. 1971. "Blasting Vibrations and Their Effects on Structures," Bulletin 656, U.S. Bureau of Mines, Department of the Interior, Washington, D.C.

Siskind, D.E., M.S. Stagg, J.W. Kopp, and C.H. Dowding. 1980. "Structure Response and Damage Produced by Ground Vibrations from Surface Blasting," RI 8507, U.S. Bureau of Mines, Department of the Interior, Washington, DC.

Standards Australia. 1983. Explosives—Storage, Transport, and Use, AS 2187.2, Sydney, Australia.

Stewart, L. (2004). "Vibratory Rollers Respond to the Need for Speed." *Construction Equipment*, October 2004. www.constructionequipment.com/buyingfile/ce04ja002.asp, accessed August 12, 2005.

Svinkin, M. R. Drawbacks of Blast Vibration Regulations. www.vulcanhammer.net/ Svinkin//BLST-CRT.pdf. accessed May 17, 2005.

Deutsches Institut fuer Normung (DIN 4150). 1986. Deutsche Normen: Erschütterungen im Bauwesen—Einwirkungen auf bauliche Anlegen, Germany.

Swiss Assocation of Standardization. 1978. Effects of Vibration of Construction, SN 640 312. Zurich, Switzerland.

VonQuintus, H.L.; Rao, C.; Stubstad, R.N.; Minchin, R.E.; Maser, K.R.; Nazarian, S.; "Non-destructive Testing Technology for Quality Control and Acceptance of Flexible Pavement Construction," Interim Report for NCHRP Project 10-54, Washington, DC, 2004.

Walker, D.; P. Turner, and M. Anderson. 1998. "What We Have Learned about Superpave." www.asphaltinstitute.org/upload/ What_We_Have_Learned_About_Superpave.pdf, accessed August 15, 2005.

Whiffen, A.C. and D.R. Leonard. 1971. *A Survey of Traffic-Induced Vibrations*, RRL Report LR 418, Transport and Road Research Laboratory, Crowthorne, UK.

Wolters, R. O. 1998. "Tenderness of Hot Mix Asphalt." *North Central Superpave Center News*, Volume 1, Number 2, Winter/Spring 1998/1999, http://bridge.ecn.purdue.edu/~spave/Newsletters/ncsc%20-%20Winter%201998-99.html, accessed August 15, 2005.